Turun yliopisto
University of Turku

OPTIMIZATION OF PORE SIZE AND THERMAL CARBONIZATION TREATMENT FOR POROUS SILICON SENSOR APPLICATIONS

Jaani Tuura

TURUN YLIOPISTON JULKAISUJA - ANNALES UNIVERSITATIS TURKUENSIS
Sarja - ser. AI osa - tom. 560 | Astronomica - Chemica - Physica - Mathematica | Turku 2017

Turun yliopisto
University of Turku

OPTIMIZATION OF PORE SIZE AND THERMAL CARBONIZATION TREATMENT FOR POROUS SILICON SENSOR APPLICATIONS

Jaani Tuura
(né Paski)

TURUN YLIOPISTON JULKAISUJA – ANNALES UNIVERSITATIS TURKUENSIS
Sarja - ser. A I osa - tom. 560 | Astronomica - Chemica - Physica - Mathematica | Turku 2017

University of Turku

Faculty of Mathematics and Natural Sciences
Department of Physics and Astronomy

Supervised by

Jarno Salonen
Docent
Department of Physics and Astronomy
University of Turku
Finland

Reviewed by

Adrian Keating
Associate Professor
School of Mechanical and Chemical Engineering
The University of Western Australia
Australia

Guiseppe Barillaro
Associate Professor
Dipartimento di Ingegneria Dell'informazione
Universitá di Pisa
Italy

Opponent

Leigh Canham
Professor
Nanomaterials for Biomedicine and Photonics
School of Physics and Astronomy
University of Birmingham
United Kingdom

Cover image by author

The originality of this thesis has been checked in accordance with the University of Turku quality assurance system using the Turnitin OriginalityCheck service.

ISBN 978-951-29-6844-2 (PRINT)
ISBN 978-951-29-6845-9 (PDF)
ISSN 0082-7002 (Print)
ISSN 2343-3175 (Online)
Painosalama Oy - Turku, Finland 2017

Acknowledgments

Little did I know, where I would be today, when I walked through the doors of Laboratory of Industrial Physics to receive the subject to my master thesis. Back then plan was simple, get the degree and go find a teacher's job. Now, way too many years from that moment, it feels that starting thesis about the subject I didn't know at all, was the best thing that could have happened to me. Naturally, one of the easiest subjects turn out to be rather complex, but still I got the degree and it is even time to show appreciation to everyone who have helped me to reach PhD.

First I would like thank my supervisor, the beloved leader of our laboratory, Jarno for his support even on this project that never seem to end. Especially, I thank him for all the fruitful discussions and far-out ideas he always has. Hopefully, after this thesis there is time to start new projects, more related to history of physics rather than contemporary research on materials. Also the closest collaborator on my articles in this thesis, Mikko has to be honored and acknowledged for his help at the infancy of my graduate student career.

I also want to express my sincere gratitude to all my colleagues, present and former, in the lab, Ermei, Mikko T., Martti, Janne, Kalle and others, with whom I have had numerous interesting discussions, some even related to research. Those not mentioned by name are still big part of our wonderful staff that is one of kind. You are all important persons to me as well. Special thanks go to Matti for his late cheers in the final stages of my thesis project.

I have been privileged of working alongside so many inspirational persons within the University of Turku, distributed to every faculties and almost each of the departments. Also with so many individuals all over the Finland have been part of this journey. Especially, Sanna M., Sanna R., Veli-Matti, Jaakko and Mikael are to be praised for their partnership in various projects. There

is still so many to whom I am indebted, so this is collective huge thanks to You all, Science teachers, students *et al.*

I would like thank pre-examiners of my thesis, Professors Adrian Keating and Guiseppe Barillaro for their valuable remarks on thesis and Dr Helen Cooper for her work checking the grammar and enhancing the readability of this thesis. I could not be more happier to welcome Professor Leigh Canham as my opponent. I am truly honoured by this opportunity to present my work to great figure from the world of porous silicon.

As time goes and persons may change, but the friendship persists. I am blessed with some of the most awesome friends, with whom you never have enough time to discuss and change the views of the World. You know who you are and my appreciation to you is immense.

Naturally, acknowledgements would be insufficient if the parents would not be mentioned. So, this is to you Kirsti and Antero, my parents who have had the patience and wisdom to guide me through difficult times and cheered when there has been time to celebrate. As well as parents, I would like thank my brothers, Jouni and Jarno, for the fights, Emilia for being the cute little sister and Niko for being the dude. I would like to thank my parents-in-law, Raija and Taisto, for their significant help during all these years and also Maiju for your her help and giving me the opportunity to pursue career in academics.

Like not knowing where I would be 15 years later, when I started my master thesis, I am again in uncharted waters. Though uncharted, I have explorer alongside with me who ascertains that the best is yet to be come. So, thank You Juliana. Last but not least, I would like to express my love and gratitude for my children, Iina and Iivo. You are the ones, that make this journey of life worth taking. The feeling of sheer joy and proudness is inconceivable to put into words.

And now "Piss off!"

Turku, May 2017 *Jaani Tuura*

Abstract

Porous silicon (PSi) is an interesting material and its use in various applications has been studied extensively. One such application is detecting humidity and gas under ambient conditions. Typically, PSi gas sensors are compromised by problems with long term stability and hysteresis. This thesis presents optimization procedures for addressing both of these problems, which are manifestations of both the silicon itself and pores in it.

Typical way of producing porous silicon is to use electrochemical etching to form nanometer size pores in to the material. These pores enlarge the surface area to mass ratio and enables the use it as a sensor material. Increase in surface area also makes the material more susceptible to ambient condition, especially to oxygen. Carbonization has been found to be sufficient way to avoid oxidation. Moreover, earlier studies have shown that thermally-carbonized porous silicon (TCPSi) can be used efficiently as a capacitive humidity sensor.

One of the optimization procedures was to determine the best possible carbonization procedure. The hygroscopicity of TCPSi can be tuned by adjusting the treatment temperature. Acetylene is used as a carbon source and also the use of acetylene during the thermal treatment has an influence on hygroscopicity.

Annealing PSi in an inert gas environment to enlarge pores was found to be an effective way of diminishing hysteresis. However, this also reduced the surface area of the pores, which in turn had a negative impact on sensitivity. Even with this reduced sensitivity the sensors showed a correspondingly faster response and exiguous hysteresis. Based on the studies on the reduction in hysteresisis, it was concluded that a hydrophilic surface and annealing are the best choices for TCPSi humidity sensors. These sensors were also tested for long-term stability. Although sensitivity decreased during storage

under ambient conditions, the overall performance of the sensors remained satisfactory.

To solve problem arising from decreased sensitivity, electrical insulation between the sensing layer and the substrate was proposed. As TCPSi is resistant against hydrogen fluoride (HF), a new porous layer can be formed underneath the previously formed TCPSi sensing layer. Several possibilities for passivation methods applicable for this porous layer exist. But for capacitive sensing, oxidation is the rational choice, because the oxidized layer will form an electrical insulation between the TCPSi sensing layer and the silicon substrate, so that the current cannot bypass via the substrate at all. Three different oxidation methods and their effect on the silicon substrate as a whole were studied. Electrochemical oxidation was found to be the most suitable method for insulation. This insulation increased the sensitivity of the sensors by more than five times compared to the original sensors.

In addition, a new carbonization procedure was introduced in the studies presented in this thesis. In this carbonization procedure two successive thermal treatments were used to obtain a more reproducible surface termination. Taking into account both the adjustment of the pore size distribution and the new surface treatments, the study shows better reliability of the TCPSi sensor in terms of negligible hysteresis without compromised sensitivity, as well as good long-term stability of the sensor.

Tiivistelmä

Huokoinen pii (PSi) on mielenkiintoinen materiaali ja sillä on useita potentiaalisia sovelluksia, joita on laajalti tutkittu. Yksi tutkimuskohteista on ollut kosteus- ja kaasuanturien valmistus. Tavallisesti huokoisen piin antureissa on sekä stabiilisuus että hysteresis ongelmia. Tässä tutkimuksessa esitetllään tapoja, joilla on pyritty poistamaan kyseisi¨ ongelmia, jotka liittyvät toisaalta piin tyypillisiin ominaisuuksiin kuin myös huokosista materiaalissa.

Yleinen tapa tehdä huokoista piitä on suorittaa sähkökemiallinen syövytys. Tällä tavalla saadaan aikaan piin n. 10 nm reikiä. Huokosten vaikutuksesta piin ominaisuudet muuttuvat sopiviksi mm. anturisovelluksiin, kun materiaalin pinta-ala kasvaa suhteessa sen massaan moninkertaiseksi. Ongelmana on näissä huokosiisa on, että samalla materiaali reagoi herkästi ympäristön hapen kanssa. Huokoisen piin karbonisaatio on yksi tapa ehkäistä ja hidastaa piin muuttuminen piioksidiksi. Aiemmissa tutkimuksissa on esitelty huokoisen piin terminen karbonisaatio, joka on osoitettu toimivan hyvin kapasitiivisena anturina.

Yhtenä tutkimuksen kohteena oli karbonisaatioprosessin optimointi. Huokoisen piin hygroskooppisuutta voidaan säätää käsittelylämpötilaa muuttamalla. Hiilen lähteenä olevan asetyleenin määrää muuttamalla lämpökäsittelyn aikana, voidaan myös vaikuttaa merkittävästi hygroskooppisuuteen.

Piin huokosten suurentaminen lämpökäsittelyllä, inertissä kaasussa, havaittiin olevan varsin hyvä tapa pienentää anturissa esiintyvää hysteresistä. Toisaalta se myös pienentää huokosten pinta-alaa merkittävästi ja siten myös anturin herkkyyttä. Kaikesta huolimatta anturin herkyys säilyi riittävänä ja lisäksi huokosia suurentamalla saatiin vasteaikaa lyhennettyä. Myös anturissa esiintyvä hysteresis katosi. Tulokset yhdistettynä todettiin lämpökäsitellyn ja hydrofiilisen anturin toimivan parhaiten anturisovelluksissa. Lisäksi tämän kaltaisella anturilla toteutettiin pitkän aikavälin tutkimus, jossa an-

turin stabiilisuutta seurattiin. Vaikka anturin herkkyys heikkeni seuranta-aikana, oli anturin toiminta edelleen tyydyttävällä tasolla.

Herkkyyden parantmiseksi tutkittiin sähköisen eristeen muodostamista anturikerroksen ja alla olevan pii alustan väliin. Tämä on mahdollista, koska termisesti kabonisoitu huokoinen pii on kestää hyvin uuden syövytyksen ja uusi syövytys ei vahingoita jo käsiteltyä kerrosta. Tämän uuden kerroksen käsittelyyn on useita vaihtoehtoja, mutta uuden kerroksen hapetus on paras tapa saada sähköinen eriste. Kolmea erilaista hapetusmenetelmää kokeiltiin ja tutkittiin niiden vaikutuksia kokonaisuutena anturin rakenteeseen sekä anturin toimintaan. Sähkökemiallinen hapetuksen todettiin olevan paras tapa anturikerroksen eristämiseen. Sähköisen eristeen avulla anturin herkkyys kasvoi viisinkertaiseksi verrattuna tavanomaiseen anturiin.

Näiden anturin toimintaan liittyvien optimointimenetelmien tutkimuksen lisäksi tutkimusken aikana optimoitiin myös karbonointimenetelmä, jossa karbonointi tapahtuu kahdessa vaiheessa. Tällä menetelmällä saatiin karbnointi varmemmaksi. Näin ollen tutkimuksessa saatujen tulosten perusteella huokoisen piin kosteusanturin ominaisuuksia parannettiin merkittävästi. Tuloksena saatiin kosteusanturi, jolla on nopea vaste, loistava herkkyys, olematon hysteresis sekä on riittävän stabiili.

List of original papers

This thesis is based on the following publications, which will be hereafter denoted as papers I - IV:

I J. Paski*, M. Björkqvist, J. Salonen and V-P. Lehto: Effects of the treatment temperature on thermally-carbonized porous silicon hygroscopicity phys.stat.sol (c), **2**, 3379 - 3383 (2005).

II M. Björkqvist, J. Paski*, J. Salonen and V-P. lehto: Studies on hysteresis reduction in thermally carbonized porous silicon humidity sensor IEEE Sensors journal, **6**, 542 - 547 (2006].

III J. Tuura, M. Björkqvist, J. Salonen and V-P. Lehto Long-term stability of thermally-carbonized porous silicon humidity sensor Mater. Res. Soc. Symp. Proc. **876E**, R8.8.1 (2005).

IV J. Tuura, M. Björkqvist, J. Salonen and V-P.Lehto: Electrically isolated thermally carbonized porous silicon layer for humidity sensing purposes Sensors and Actuators B-chemical, **131**, 627 - 632 (2008).

Contents

Chapter 1

Introduction

1.1 Porous silicon at a glance

Porous silicon (PSi) is a derivative of silicon (Si), which is anodized electrochemically to obtain a porous substance [1, 2]. Pores in PSi are usually mesoporous for p-type Si, based on the IUPAC classification [3], 2 - 50 nm in diameter. Also macropores from 1 μm to a couple of dozens of micrometers are feasible in n-type Si [4–6]. The pore region ranging from 50 - 500 nm remained unstudied until recent interest in intermediate pores [7, 8] The porosity of PSi notably changes its properties compared to Si, the surface area increases significantly after anodization even to several hundreds of m^2/g [9]. This increase in surface area promotes the use of PSi as a sensor material [10]. Due to the pores incorporated into silicon, PSi exhibits interesting properties related to dimensions in the material. While silicon itself is luminous at temperatures of liquid helium (5 K) [11] PSi is luminous even at room temperature [12, 13]. This luminecence is due to quantum size effects in the PSi matrix [12, 13].

Interesting occurrences, which become perceptible at the nanoscale, are the driving force for an ever increasing interest for this versatile material. The next paragraphs will describe in more detail the history and the current applications of PSi.

1.2 Historical overview

More than half a century ago A. Uhlir [14] and co-workers were studying the electropolishing of germanium and silicon. They found that electropolishing in hydrofluoric acid (HF) results in a matte black, brown or red deposit. They concluded that the outcome was due to the electrochemical oxidation of the silicon. Later, Turner [1] carried out more detailed studies on the electropolishing of silicon in HF, especially under conditions where a solid film is formed, and observed the same deposit as was seen by Uhlir in his studies. Turner also found that solid films were explosive when they came in contact with strong oxidizing agents. Turner also reported the possibility of removing the solid film by increasing the current above a critical value, where the electropolishing starts. Like Uhlir, also Turner discovered that the density of the solid films is less than that of bulk silicon. Turner pointed out in a text that the film is probably porous, but the true composition and nature of the anode films were only assumptions at the time. The composition of the anode films was defined by infrared spectroscopy (IR) as it became a common research method at the start of the 1960's (based on a database search of IR spectroscopy [15]). Beckmann [16] was the first to apply this method to anode films of silicon. From these studies he concluded that the film is mainly composed of silicon hydrides instead of silicon oxides. Later Memming and Schwandt concluded that the silicon etched in concentrated HF solutions was very porous [17]. They also produced a respectable formation model of the anode film, which has since been replaced by a more precise model. Formation models are discussed later in the text.

The term Porous silicon was adopted presumably by Watanabe and Sakai [18]. Although, "*anode film*" was still used in the title of the article. Overall, the research on PSi was motivated from the very beginning to the end of 1980's by its potential use in integrated circuit (IC) technology [14, 19, 20]. Especially, in silicon-on-isolator technology to obtain high quality thick oxide layers [20–22]. There was also an increasing interest to understand the formation mechanism [20, 23–26] as well as the porous nature and the porosity [27–31] of PSi.

It wasn't until 1990, that the photoluminescence of Psi at room temperature was observed [12, 13]. This then increased the interest in PSi more widely. Consequently, the discovery of the photoluminesence in PSi was preceded by Canham's work on hydrogen implantation to crystalline silicon and

its photoluminescence [32, 33]. Other observations on both the chemi- and electroluminescence of Psi soon followed [13, 34–37].

As the interest spread, the need to understand the formation of PSi arose and several new studies on the dissolution reaction were published [38–51], Lehmann *et al.* presented the chemical reaction for PSi, described in Fig. 1 [13], which is a defined scheme of a model proposed earlier by Memming and Schanwdt [17]. While the chemical reaction at the interface of Si - HF has been generally approved, a uniform model for how pore growth is initiated and sustained at the pore tip is still under scrutiny [6, 52], though recently Foca *et al.* have presented a thorough study in favour of a current burst model (CBM) [53]. Earlier Parkhutik *et al.* had developed a general formation process for porous materials, which has been ignored in the field of PSi research, but has found foothold in other disciplines [54].

Canham's discovery started a new era in the research of PSi based on its luminescence. Also research on stabilizing the material for prolonged and more effecient luminscence began[55, 56], as it was clear that silicon hydrides at the interface of a large surface area are extremely unstable. Also, some research groups began to exploit the large specific surface area of PSi in sensing applications [10, 57–61].

The first hydrosilylation studies from the break of the new millenuim [62, 63] opened the door for a vast expansion in surface treatments based on silicon - carbon bonds. These first treatments paved the way also for more sophisticated surface treatments used nowadays especially in bioapplications [64–67]. At the moment, Psi is used in diverse applications in several different fields of science, which are covered in next section.

1.3 Contemporary applications of porous silicon

Studies on the applications of PSi started from a desire to develop better semiconductor interfaces [14], soon followed by applications in integrated circuit technology [18, 19, 68, 69] in materials first decades in use. But major advances were made after the exploitation of quantum size effects in PSi [12, 13]. Nowadays, the applications based on PSi range from thermoelectric generators to nutritional additives [70, 71]. As the potential and list of applications are nowadays so vast, only a selection is covered in this thesis.

After the discovery of the luminescence in PSi, its optoelectronic applications were intensively studied [61, 72–77]. However, poor quantum effiency (QE) and instability of the luminescence soon started to reduce the interest towards PSi in optoelectronic applications [78]. The introduction of surface terminations that sustain luminescence, silylation and metal deposition on PSi surfaces, has somewhat rejuvenated the research field in the 21st century [79–83]. Along with new surface chemistries on PSi, also enhanced production procedures have been adapted to better control the nanoscale structures responsible for the luminescence [84]. Other optoelectronic novelties have accompanied Psi, such as Si nanoclusters and nanowires [85, 86]. PSi has also found use as a template material for other optoelectronic composites [84].

Soon after the room temperature luminescence was reported, the first possible bioapplications based on PSi were introduced by Canham [87], in a study of apatite nucleation on PSi. Previously, SiO_2 and CaO based bioglasses were reported to promote the growth of apatite on simulated body fluids [88]. Nevertheless, Canham's original study expanded the research on PSi into the new fields and bioapplications started to surface [89–93]. The use of PSi as a biomaterial is inspired by the possibility to adjust it to be either inert, active or degradable in accordance with its porosity or surface chemistry [64, 94–103]. Bone tissue engineering by PSi is well documented and is still studied [104–109].

Like in the case of other Psi-based applications, the use of PSi as a drug delivery vehicle has been inspired by the earlier use of silicas for the same purpose [110, 111]. Zangooie *et al.* were the first to report protein adsorption in oxidized PSi layers [112]. Few years from this discovery, the first reports on PSi-mediated drug delivery were published [98, 113–115]. Soon after this PSi was established as an attractive material for any drug administration pathway [102, 116–118]. The key to the vast interest in PSi in drug delivery applications is in its ability to sustain or accelerate drug release [116, 119–121]. Versatile surface chemistries along with a tuneable pore morphology, complemented by adjustable particle size and *in vivo* characteristics, PSi has a lot to offer for future drug administration technologies [99, 100, 122–132].

Gas and bio sensing are among the strongest research branches involving PSi. The first reports on the electrical characteristics of Psi were published as early as 1990 was by Anderson *et al* [10]. Their design for a PSi gas sensor was striated-mesa with aluminium contacts. The device showed an adequate response towards both humidity and ammonia vapour [10]. After

the luminescence was observed, reports on quenching of the luminescence and especially quenching due to different adsorbates started to appear [133–136]. But it took another few years until this quenching phenomena was actually referred to as sensor behaviour [137, 138]. Yet again the progress in surface treatments has led to better durability and selectivity in PSi sensors [139–143]. As it is applicable to control the porosity of PSi during etching, different types of reflectors were adopted for sensing purposes [112, 144–146]. At first they were simple Bragg reflectors, but as the manufacturing procedures developed, new more complex reflectors became feasible [147–150]. Sensor development on PSi sensors nowadays include printable gas sensors [151, 152], composite sensor structures [153, 154] and electrostatic sensors [155]. While the performance levels of PSi sensors are promising, polymer or ceramic based humidity sensors are still used commercially because of the cheaper price combined with adequate performance [156]. Lately, with the miniaturizing of such sensors, also hysteresis has been suppressed to an appropriate level [156].

Fuel and solar cells as well as battery technologies based on PSi have attracted a lot of attention in the past few years [157–159]. In battery applications Si possesses a better power storage capacity than other applicable materials [160, 161]. There are still issues with PSi battery technologies [161, 162], but batteries are among the most promising applications of PSi. The use of PSi in fuel and solar cell technologies is reported in "Handbook of Porous Silicon" [163–165]. PSi is found to be a good template or sacrificial material in various applications [166–169].

Chapter 2

Fabrication and stabilization of porous silicon

2.1 Fabrication of porous silicon

PSi can be easily fabricated with a simple electrochemical etching unit or cell [170, 171]. The cell consists of an anode electrode, normally a silicon wafer itself, a cathode electrode, preferably platinum, and an aqueous electrolyte, which can contain various concentrations of hydrofluoric acid (HF), see figure 2.1. In addition to simple electrochemical etching, there are several other methods for producing pores in Si, and descriptions of these methods can be found in the literature [170–176]. Different surfactants are added to the electrolyte to diminish surface tension and to reduce the formation of bubbles during etching [170, 171]. As it is possible to etch pores into Si with a variety of electrolytes, with or without illumination and even with more or less continuous current densities, the outcome is that pore formation and the size of the pores can be adjusted depending on the desired characteristics of the PSi [171, 177].

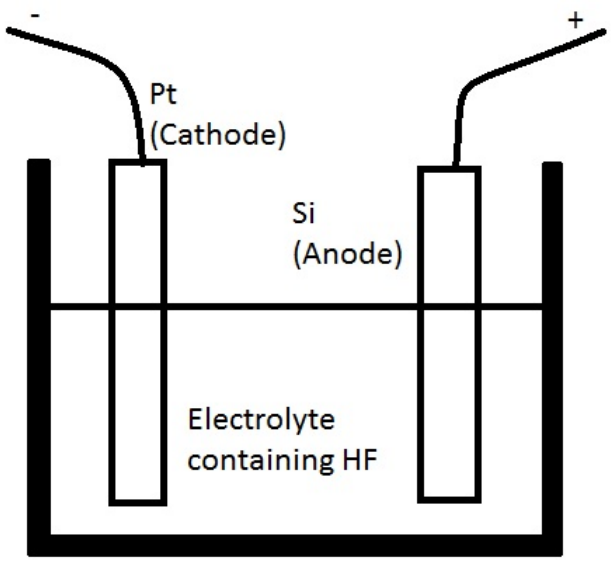

Figure 2.1: A simple anodizing cell is presented.

In the case of n-type silicon, the use of light to initiate pore propagation on the surface is extremely important, whereas light is seldom used for p-type silicon, though it has a distinctive effect on pore propagation [178, 179]. This is due to different charge carriers in p- and n-type silicon. As the main charge carriers in n-type silicon are electrons, the intrinsic hole concentration is low. However, with a dopant, the anodization conditions can be changed and even n-type Si can be anodized without light [170, 171, 177]. Normally for n-type Si, pore formation is initiated by a hole injection on the surface of the silicon and this hole injection can be facilitated by light [1, 17, 177, 180].

As was mentioned earlier, the anode reaction leading to pore propagation in bulk Si is widely approved. In figure 2.2 the reaction is shown as it was presented by Lehmann and Gösele [13]. A more precise model is proposed by Kolasinski [52], but Lehmann's model is adequate for most purposes. The divalent dissolution leads to pore formation, whereas the tetravalent reaction leads to electro-polishing of the Si surface [13, 177].

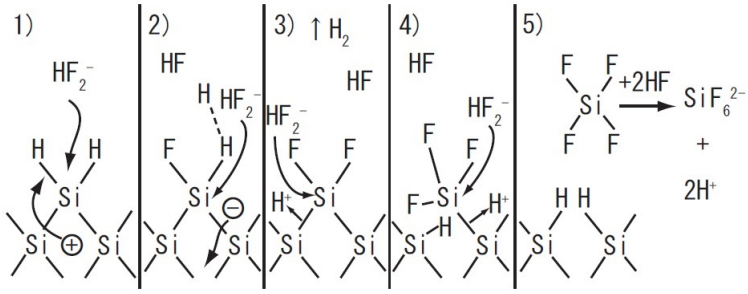

Figure 2.2: Reaction of Si in HF electrolytes proposed by Lehmann. Image taken with permission from [13].

2.1.1 Structure of the porous layer

In the previous section it was noted the different ways of producing Psi are almost endless. This leads to very different kind of pores and pore morphologies depending on etching parameters [6, 170, 171]. In general, n-type Si leads to a macro-porous and p-type to a mesoporous layer [6, 181], and an increase in the dope concentration increases the pore size for the p-type and decreases it for the n-type [171]. Aforementioned rules apply to the case where simple aqueous HF electrolytes have been used for etching [182]. Additives in the electrolyte, surfactants *etc.* have their own specific impact on the resulting morphology, especially on the branching of the pores [6].

Overall, the pore size and morphology can be altered in a very wide range from micropores to macropores, from sponge-like, highly interconnecting pores to a smooth, columnar pore structure. Even surface areas can be tuned by changing the pore morphology from smooth pore walls to a branching, fir-tree type morphology. All of these can be achieved by simply changing the type of the initial Si and the etching parameters.

Pore propagation has been found to prefer the $\langle 100 \rangle$ crystallographic direction [6, 181]. Thus, pores propagate perpendicular to the surface in (100) oriented substrates. Moreover, on other plane orientations, the same behaviour has been detected and pores will try to form in the $\langle 100 \rangle$ direction [177, 183]. Another preferred orientation is $\langle 113 \rangle$, which can be seen on branches of the main pores and in cases where the electric field is applied along the $\langle 111 \rangle$ direction of the Si substrate, figure 2.3 [183].

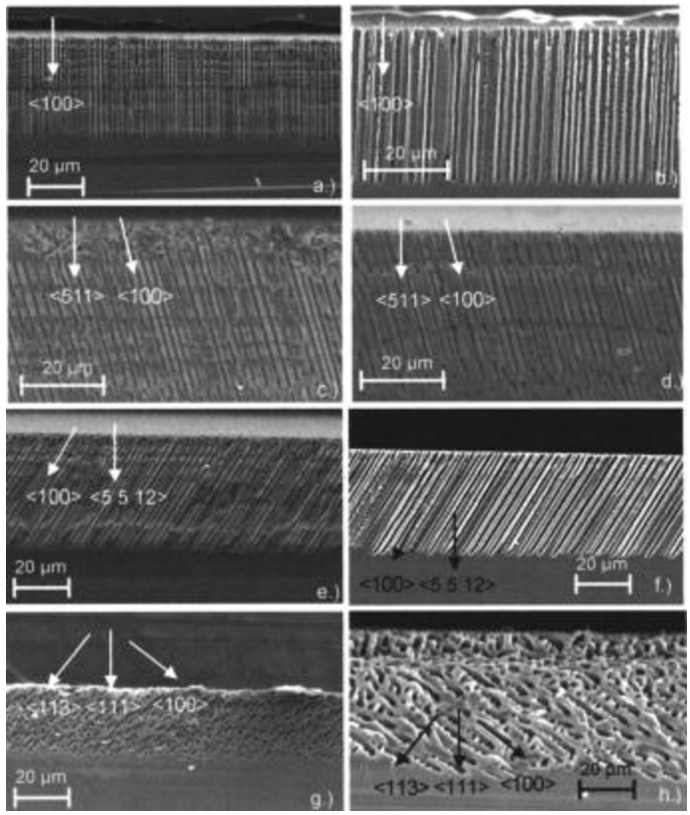

Figure 2.3: Propagation of pores in various crystal orientations by Christophersen *et al.* with permission from [184].

One of the benefits of PSi is that its pore structure can be modified during etching. Surface active species can be added into the electrolyte, illumination conditions can be changed *etc.* [181]. However, changing the current density is the easiest and most precise technique for modifying pore structure during etching. This is the key for the use of PSi as an optical filter and even extremely complex structures like rugate optical filters can be produced from PSi [170]. For simple reflectors two current densities are applied consecutively for several times to produce variations in the refractive index and based on these changes the optical path of light can be changed [147, 185]. For more complex structures, the current density can be modulated with a sinusoidal profile to obtain rugate filters [186–190]. Figure 2.4 presents some of the pore structures obtained by modifying the current density during anodization. In this case, also the surface chemistry of the different layers are different, the

upper part being a hydrophilic and the lower part a hydrophobic layer [191]. Modifications to the surface chemistry will be discussed in the next chapter.

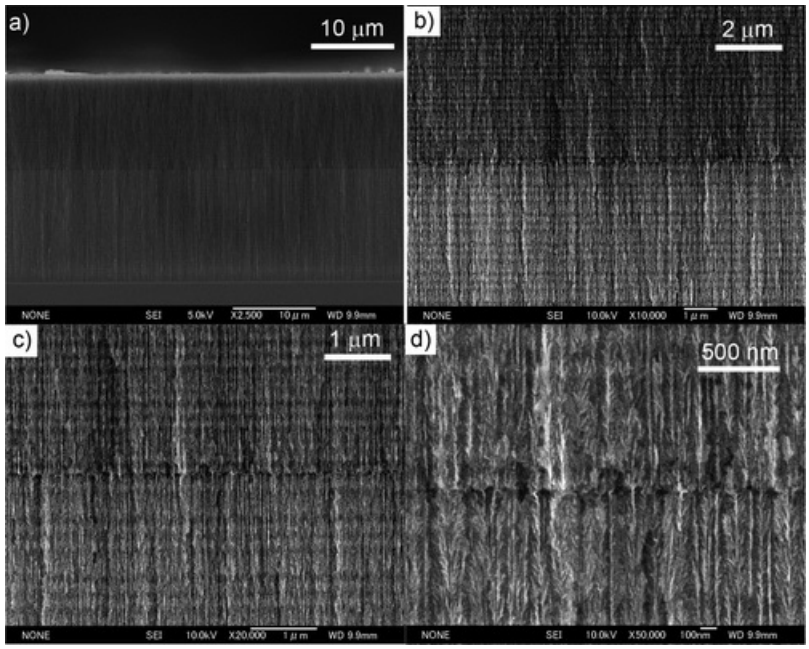

Figure 2.4: Stacked rugate mirror with two different reflectance wavelengths and surface chemistries to promote selectivity of the sensor structure. Image taken with permission from [191].

2.1.2 Formation models

While the dissolution reaction of Si in HF containing electrolytes is unanimously accepted, a general model for explaining the formation of the pores has not been agreed on. This is due to the numerous pore morphologies and sizes found in PSi. Several models have been suggested in the past, but they fail to give an undisputed explanation for the different pore structures obtained in PSi [13, 25, 26, 38–40, 47, 48, 52, 78, 181, 192–195].

The first quantitative model for pore growth was introduced by Beale *et al.* Their model is based on the observation that pore walls are inert to an anodic attack after the pore has formed and also the resistivity of the porous layers was significant compared to the Si substrate. This leads to a model as follows: The material is dissolved from points where current flows and a

large surface state density in the porous film of Si results in pinning of the Fermi level. Therefore, pore growth propagates from the pore tip instead of the pore walls, as charge carriers have been depleted from the walls. [25, 26]

The diffusion limited model is based on the random walk of the holes in Si, but as this relies on diffusion in the anodized material, it lacks the chemical species of the reaction. Therefore, the diffusion limited model is insufficient to predict PSi pore formation in practical applications. [6, 39, 181, 192]

Lehmann and Gösele found out that the band-gap of the Si increased in walls according to diminishing wall thickness. This led to the conclusion that a quantum confinement effect in pore walls inhibits the hole diffusion and limits the pore growth in the horizontal direction of the pore axis [13]. This model was later adjusted by Fronhoff *et al.* [45]. A problem of this model, even with modification, is that it gives precise distances of the pores but fails to give variation in the size of the pores [6].

The recent current burst model (CBM) presented by Föll *et al.* has established itself as the most comprehensive formation model and several studies on its application in predicting pore morphology have been published [53, 196]. CBM has some resemblance to the unnoticed model by Parkhutik *et al.*, the virtual passive layer (VPL) model [78]. In both models, pores grow as a dissolution of the passive layer. CBM is based on oscillation, which was first observed by Chazalviel *et al.*. They also proposed the existence of micro-oscillations on the electrode [197] As CBM is a Monte Carlo simulation based on oscillations found during etching, there are limitations to sample sizes that can be modelled with CBM [53].

2.2 Surface passivation of porous silicon

After anodization, the surface of the PSi is covered with SiH_x, but this termination is unstable. As is seen everywhere on Earth, Si is naturally bound to oxygen, forming silicon oxide (SiO_x). This tendency of Si to oxidise has been inhibited in the case of PSi by various stabilization methods. Stabilization of the PSi can often be seen as a functionalization, as new applications commonly arise from the new surface chemistries.

Oxidation

Oxides naturally form on Psi, and this phenomenon is usually undesired in Psi-based applications. On the other hand, oxide formation can be utilized for creating a more stable surface, as the outcome of the oxidation depends on its mechanism [19, 23, 198–202]. Oxidation methods can be divided into three groups. Thermal oxidation is commonly used and various means of thermal oxidation have been developed [55, 199, 203–206]. Chemical oxidation is typically carried out within temperatures of liquid water and includes a reactant or catalyst, so that the chemical reaction resulting in silicon oxide can occur [201, 206–211]. As its name implies, electrochemical oxidation stands for a process where an electric field is applied to form an oxide [35, 56, 177, 212].

Before room temperature photoluminescence was observed in PSi, the full oxidation of the PSi layer was a desired property for electronic applications. After Canham's discovery, oxidation was briefly seen as an undesired property until photoluminescence was found to persist even in oxidized PSi [55]. A common feature of oxidation during this era was the use of high temperatures in either a dry or humid atmosphere [19, 55, 213].

The application usually determines the thermal oxidation method used. For fully oxidized PSi, the use of high temperatures and relatively long treatment times are required [20, 23, 203]. For sensor applications, the same oxidation procedures can be used as in the case of SOI applications [140, 214]. In the case of luminescence, thermal oxidation may also enhance the intensity of the luminescence in the long run [55, 205].

In thermal oxidation, the oxygen from the ambient surroundings reacts with PSi to form various compounds with Si, like siloxane and silanol [23, 206, 214, 215]. Oxidation occurs even at RT, so the actual temperatures for thermal oxidation range from 20 - 1200 °C. Oxygen will be more likely to affect the Si - Si bond at the very surface, break it and reside in that position [216]. Increasing the treatment temperature enhances the incorporation of the oxide into the silicon structure [23, 216, 217]. Naturally, the treatment time also affects the incorporation of the oxide to a certain extent [213, 218, 219].

As in the case of thermal oxidation, also chemical oxidation includes various alternative procedures for achieving oxidation [201, 209, 220]. In general, PSi can be chemically oxidized just by adding a reductive agent with water and immersing PSi into the solution. Typically, the applied reagent for oxidation is either H_2O_2 or HNO_3 in aqueous solutions [206, 207, 221]. Chemical oxidation can also be achieved by using a catalyst like pyridine

to obtain oxidation, this oxidation procedure requires water vapour as an oxidant [201, 210]. Also, the use of ozone has been reported [221] as well as dimethyl sulfoxide (DMSO) [117].

Electrochemical (anodic) oxidation requires a simple set-up of electrodes with a power supply and an electrolyte. The electrolyte can be in principle any diluted aqueous salt or acidic solution *ie.* H_2S_4, KNO_3 or HCl [35, 212, 222–225]. The current density is maintained at a considerably low level compared to etching [212], this is done to obtain a uniform SiO_x-layer. With increasing current densities or decreasing doping levels of the material, the oxide will grow from the bottom of the porous layer and eventually stop and no further oxidation will occur [226–228].

Although the chemical and electrochemical oxidations methods are not compatible with most of the currently used microelectronics fabrication methods due to potential contamination issues, they may offer a good choice for other applications. All of the three oxidation methods were considered in the studies of this thesis.

Organic derivatization and thermal carbonization

Covalent silicon - carbon bonds, both organic and carbon alone, were first demonstrated for plain silicon surfaces and eventually adopted for the PSi surface [62, 63, 229–235]. The use of organic derivatization and carbonization has opened the door for new applications for PSi as presented in earlier sections. Buriak *et al.* first announced the Lewis acid mediated hydrosilylation of PSi, where they introduced alkene and alkyne terminations to PSi [234]. Another route for alkyl termination for PSi was reported by Boukheroub *et al.* Their approach was to thermally induce the reaction between the PSi surface and various organic molecules [63, 236].

Both routes lead to a mono-layer of organic species on the surface of the pores. Due to the characteristics of the alkene chains there is still plenty of H terminated surface states present after the production of the derivatized surface [237]. Nevertheless, these treatments increase the stability of the samples several orders of magnitude compared to H-terminated surfaces [64, 117].

One notable surface treatment of PSi, which has shown extremely good resistivity against any corrosives, is thermal carbonization [140]. Salonen *et al.* showed that carbon can be bonded to the surface of PSi [235, 238, 239]. This process used the property of acetylene (C_2H_2) to adhere to the

surface of Si and react with the Si surface. It has been studied during recent decades and several studies have been reported [229, 230, 239–242]. Different procedures for thermal carbonization have been tested. For PSi, the original procedure was as follows [235]:

1. Fresh as-anodized PSi sample is placed in a quartz tube and an inert gas flow of nitrogen is added and kept for 30 min.
2. Acetylene flush is added to the gas mixture for 15 min.
3. Acetylene flush is removed
4. Before the PSi sample is placed into the furnace, the short delay time was used to let surplus acetylene flow out from the quartz tube
5. Sample is kept at a steady temperature of 820 °C for 10 min.
6. After the thermal treatment, the sample is left to cool inside the tube under a nitrogen flow

Naturally, several different temperatures have been tested, ranging from 425 - 930 °C [235, 238, 239]. Based on these studies, it was shown that a significant change takes place in the surface chemistry at around 700 °C. For treatment temperatures below 700 °C, the surface is hydrophobic, whereas above 700 ° the surface becomes hydrophilic. Also, Fourier transform infrared spectroscopy (FTIR) indicated clear traces of hydrogen on a surface in the former case but no such traces in the latter. From previous studies it was known that such a transition should occur [240, 241]. In short, at a transition temperature regime, carbon will incorporate into to the Si substrate as acetylene decomposes. Moreover, hydrogen desorbs at the same time. A possible surface composition for Si-C-H (hydrosilylated surface) is presented in Fig. 2.5. In the case of Si-C (Silicon carbide surface) there has been an indication of a possible C-O or Si-C-O hybrid [235, 239, 240].

One of the biggest advantages of carbonization or hydrosilylation, is that the material remains mesoporous and the surface area is diminished only slightly, whereas most oxidation methods will delete practically all mesopores from the sample [140, 239].

During the last decade Si-C based surfaces have been extensively studied and new functionalization methods have arisen from these studies. These methods have opened new bioapplications for PSi, like drug delivery vehicles

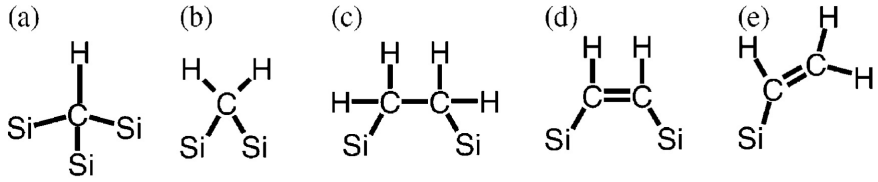

Figure 2.5: Proposed compositions for hydrosilylated surfaces, modelled based on absorption peaks in FTIR measurements. Image taken from [239].

and biosensors [243–246]. Other prospects for carbon surfaces include battery or supercapacitor applications, as reports show that these Si-C structures have a significantly higher charge density than *ie.* Li batteries [247, 248].

Other passivation techniques

Instead of using oxidation or carbon based stabilization methods, a few other strategies can be applied. One notable method is to use nitridation for passivation. Nitridation is used for integrated circuit manufacturing as an etch stop or dielectric layer [245]. With nitridation a highly stable surface and durable material is achieved, but the loss of surface area in the pores is diminished dramatically, especially during high temperature treatments [245]. Usual the routes for producing nitride passivation involve either NH_3 or N_2 atmospheres and relatively high temperatures [249–251].

Chapter 3

Sorption on porous solids

3.1 Sorption

The surface of a solid material has a unique character due to the energy of state of the atoms at the boundary [252]. Reactions are enabled by this same property. Porous silicon itself is a manifestation of the energy of state at the boundary. Sticking molecules to the surface of the Si, followed by a chemical reaction, restructures the surface and gives new features to the material. In this chapter, the physical adsorption, physisorption, is presented in more detail, especially for solid - gas interfaces.

The starting point of the sorption is rather simple, the molecules in the gas or liquid phase simply adhere to the surface. But when considering physisorption at equilibrium and how the equilibrium is achieved, especially for porous substances, sorption becomes rather complex.

The following chapters, introducing the concept of sorption, are combined from Refs. [252–257]. One important concept when dealing with physisorption is the time that it takes for a single molecule to be at rest on a surface. Now, when the molecule hits the surface it stays on the surface for some period of time and for a vast number of molecules this becomes an average time of stay (τ). If the rate of colliding molecules is greater than the rate of detachment of the molecules, then the number of molecules on a surface will increase until both rates are equal, so that an equilibrium is reached. Again, if the rate of collisions is further increased, vapor pressure is increased, the number of adhered molecules will at some point result in the coverage of molecules across the entire solid surface, as the solid material has only a

limited surface area and gas molecules have a definite size. Now, if the single monolayer of molecules covers the whole surface, the adsorption is known as Langmuir's true adsorption. This is the case normally in chemisorption and with a few physisorbed gases [252, 256]. The case when molecules start to form a second and consecutive monolayer before the first monolayer fully covers the surface, is a more common event. This is the general case of physisorption.

The difference between chemical and physical adsorption can be expressed with the average time of stay, τ, as well. In the case of physisorption the τ is usually from 10^{-10} s onwards, but when τ is more than 10^{-7} s one can consider the adsorption to be chemisorption. The time limit for physisorption is actually the minimum time at which the adsorption can happen. Another way of defining the species of adsorption, is to consider the τ as a function of interaction energy Q (or adsorption energy)

$$\tau = \tau_0 e^{\frac{Q}{RT}} \tag{3.1}$$

where T is absolute temperature, R is the gas constant and τ_0 is within the range of $10^{-13} - 10^{-12}$ s. So that an increase in the interaction energy increases τ.[252]

The origin of the adsorption energy lies in ubiquitous van der Waals forces. While travelling in a gas phase, a molecule is quite undisturbed by the other molecules in the gas phase. But relatively close to the solid surface the changes in the molecules' dipole moment causes the polarization of the solid. Dipole moment changes are due to electron motion in a molecule or atom [255]. Upon this polarization, an interaction between a solid material and a molecule is established and the adsorption can take place [258, 259]. Consecutive layers are adsorbed by the same forces that enabled the first monolayer to be adsorbed [260].

A solid surface has a definite surface area and therefore only a limited amount of sites for molecules to be adsorbed. Adsorption sites might also have different energy states depending on the molecules and the structure of the surface. Also, surface roughness affects the energy states and therefore the adsorption. According to Condon, there are no specific sites for molecules to be adsorbed in the case of physisorption [256]. Ordinarily, adsorption models are considered for the equipartition of the energy of state on a plain surface. This is a result of statistical averaging of the parameters for large

surface areas and vast numbers of molecules. Even for porous solids this averaging is justified at the macroscopic scale.

3.2 Sorption isotherms

The amount of the adsorbed vapor as a function of partial pressure p/p_0, at a constant temperature determines the isotherm of sorption. Depending on the adsorbent and the adsorbate different types of isotherms can be obtained. According to Brunauer *et al.* isotherms are divided into 5 categories [256, 258]. Later Gregg and Sing proposed isotherm type VI to be added to the isotherm classifications to complete observed isotherms [261]. Type VI is omitted in this text, as it is a special case where both chemi- and physisorption take place.

Type I isotherms, figure 3.1 are usually associated with adsorption on microporous solids and with chemisorption. Adsorption resulting in this type of an isotherm is called Langmuir adsorption, which typifies the true adsorption introduced by Langmuir. In the previous section, the Langmuir adsorption was assumed to take place first, so that after the first monolayer molecules will rebound from the surface [253]. In the case of micropores, the pores are too narrow to promote consecutive condensed layers. These types of isotherms have little use concerning mesoporous solids and therefore a more detailed discussion is ignored.

Type II and III isotherms are assigned to non-porous substances and the difference is based on the adsorption energy. The type II isotherm is for a high energy adsorption and type III for low adsorption energies [256, 258].

Type IV and V are related to isotherms for mesoporous solids. Depending on the adsorption energy, the isotherm is either type IV or V. The first is for a high energy and the second for a low energy case. In these isotherms, hysteresis becomes evident due to condensation into the mesopores of the material. A hysteresis loop gives important information about the pores and pore morphology. Hysteresis loops are categorized into 4 types, where type H1 is connected to regular even pores without interconnections between the pores. Materials, which experience type H2 hysteresis, usually have narrow and wide sections in the pores as well as possible interconnecting pores. Types H3 and H4 are typical for slit like pores, which normally would have a isotherm of type II or I, respectively. In figure 3.2, typical hysteresis loops are presented according to Condon [256].

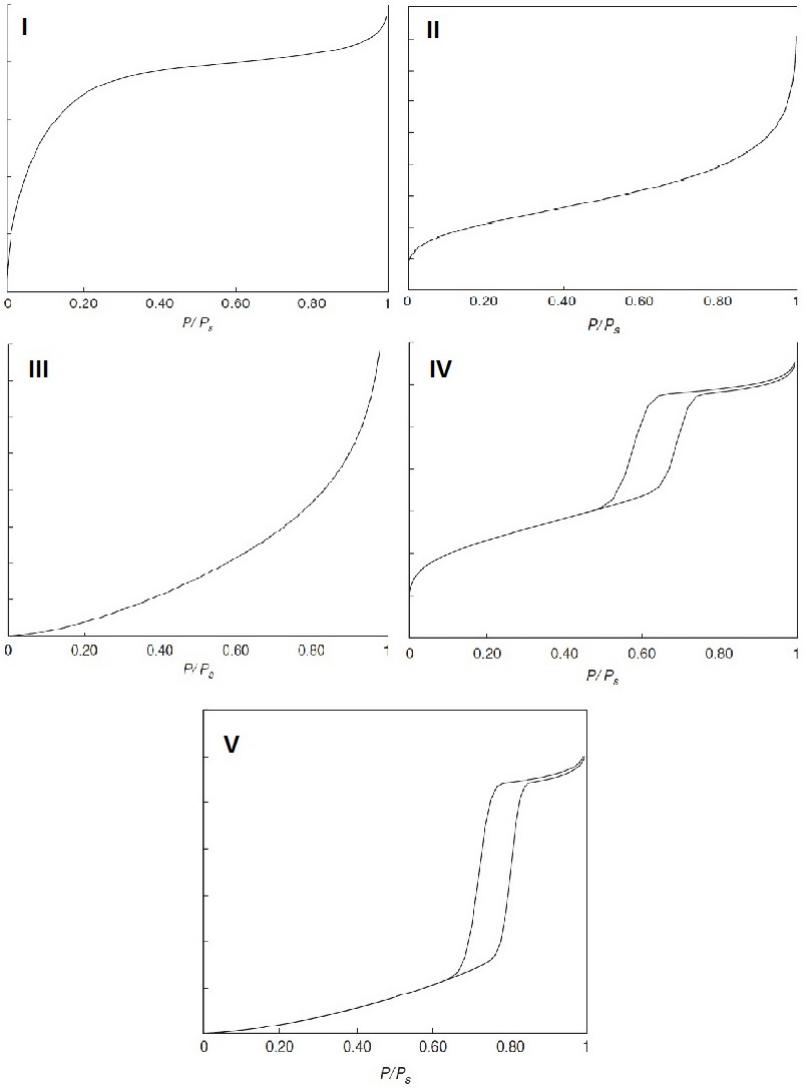

Figure 3.1: Typical classification of the sorption isotherms, from top left to bottom I, II, III, IV and V. Images taken from and presented as they were in [256].

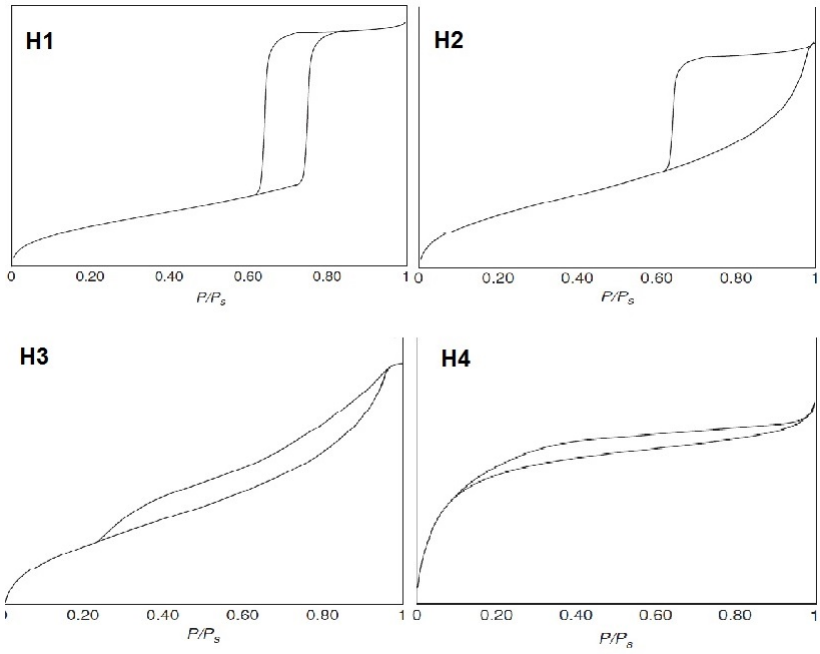

Figure 3.2: Four hysteresis types present in isotherms with characteristic delayed desorption. Images taken from and presented as they were in [256].

In summary, in adsorption studies of PSi, type IV or V isotherms along with either H1 or H2 hysteresis loops are usually detected [28, 31].

3.3 Mathematical interpretation of isotherms

3.3.1 Surface area determination

Langmuir presented the first mathematical model of adsorption for isotherms of type I. It follows the principles presented in the previous section. Langmuir used a kinetic gas theory to derive an equation for the surface coverage of the condensed gas

$$\theta_1 = \frac{\sigma_1 \mu}{1 + \sigma_1 \mu} \tag{3.2}$$

where $\sigma_1 = \frac{\alpha}{\nu_1}$ denotes the relationship between the adsorption and desorption rates, and μ presents grams of gas molecules striking against the surface in a second [253]. The current form of the equation is presented in terms of pressure p and constant K, which has essentially the same meaning as was denoted for σ_1 before. This model is suitable for those cases where adsorption sites are limited on a surface and only one monolayer is formed, as in the case of chemisorption [252]. Langmuir derived mathematical models for other adsorption processes, but the starting point for each model is a limited number of adsorption sites on a surface. Therefore, it is needless to cover other models in this thesis.

Brunauer *et al.* provided a general model for determining the surface area of the substance [260]. This model also takes into account pressures near the saturation pressure, so that the formation of multimolecular layers can be described. An important result of the generalized Langmuir's theorem is the following equation [260]

$$\frac{P}{v\,(P_0 - P)} = \frac{1}{v_m c} + \frac{c-1}{v_m c} \times \frac{P}{P_0} \tag{3.3}$$

Where v_m presents the volume of the unimolecular layer of the gas, which covers the entire surface of the adsorbent. In addition, P and P_0 are the prevailing and saturation pressures, respectively. The constant c stands for E_1 - E_L, the difference between the average energy of the first adsorbed layer and the average of the adsorption energy of the consecutive layers, the energy

of liquefaction [260]. From the adsorption isotherms it is possible to solve E_1 and v_m by a simple method of using the linear part of the graph, the former from the slope of the graph and the latter from the intercept at the vertical axis. The BET theory works sufficiently, if the surface area is determined from the part of the isotherm where the partial pressure is within 0.5 - 0.35. The BET model is still the most important model for determining the surface area of solid materials and adsorption energies [256].

3.3.2 Pore size distribution from isotherms

While the BET-model is adequate for determining the surface area, it lacks information on the nature of the pores, except the total surface area. Pore volume and further, the size distribution of the pores can be solved by applying the Kelvin equation. The Kelvin equation illustrates the condensation into pores with a radius of r at a certain pressure P. Several forms of the equation are found in the literature depending on the year of publishing, but the following equation is adopted from Cohan with modifications by Lowell and Shields [255, 262]

$$\ln \frac{P}{P_0} = -\frac{2\gamma \bar{V}}{rRT} cos\theta. \tag{3.4}$$

P stands for the equilibrium pressure in a narrow pore with a radius of r and P_0 is the equilibrium pressure at a plane bulk surface, also noted as the saturation pressure. T is the absolute temperature, γ is the surface tension of the liquid and $\bar{V}$ is the molar volume of the liquid. One important factor, a contact angle θ, stands for the extent of the wetability of the substance in the case of the adsorbate. The contact angle will be presented in more detail later in this thesis. In the case of adsorption isotherms, the θ is expected to be 0°.

The simplest prediction of the pore size distribution (PSD) in a material can be expressed with the Kelvin equation. The Kelvin radius is solved from the equation relative and the incremental volume for a certain pore size is expressed according to the total pore volume. The relative pressures are substituted with the equivalent Kelvin radius and the adsorbed volume of the gas is expressed according to pore volumes of the solid material [263]. This is naturally a rough estimate, as the Kelvin equation supposes condensation and it has been shown by Harkins and Jura, that such condensation will start only at high relative pressures [264]. The first noticeable pore size distributions

were calculated by Oulton and a bit later by Schull [263, 265]. Oulton already pointed out that the PSD should be calculated from the desortion branch, if one uses the Kelvin equation [263]. While Oulton applied a thermodynamic approach, Schull used the following equation as the basis of his calculation

$$V_s - V = \int_{r_{P_n}}^{\infty} (r-t)^2 L(r) dr \tag{3.5}$$

In this case, V_s is the volume of the gas adsorbed at the saturation pressure, V is the volume of the gas adsorbed at pressure p, $L(r)dr$ denotes the total length of pores whose radii fall between r and $r+dr$. r_{P_n} is the critical radius for the largest pore that is still completely filled with a liquid adsorbate at any particular pressure and t is the multilayer thickness of the adsorbate at pressure p [265, 266]. One of the problems with Schull's approach is that he assumed the pore sizes to follow a Gaussian or Maxwellian distribution [265]. Later Barret, Joyner and Halenda defined the model to take into account several issues regarding the adsorption and desorption [266]. To better apply equation 3.5 to obtain the PSD, one needs a set of pressure decreases and resulting volume decrease for the material to be known. Hence, multiple summations have to be made consecutively to solve the PSD [266]. Fig. 3.3 shows the idea behind the summations. The first three pressure decreases are shown and their effects inside different pore diameters. The first step diminishes the thickness of the adsorbed layer by Δt_1, which in turn increases the inner capillary radius r_{k1}. For this step it is possible to solve the pore volume of the pores with a radius r_{P1} according to the measured desorbed volume ΔV_1.

$$V_{P1} = R_1 \Delta V_1, \tag{3.6}$$

where $R_1 = r_{P1}^2/(r_{k1} + \Delta t_1)^2$. A generalized expression for any stepwise desorption can be written as

$$V_{\Delta t_n} = \Delta t_n \sum_{j=1}^{n-1} A_{cj} \tag{3.7}$$

Δt_n and A_{cj} stand for any stepwise reduction in thickness or average area from where the adsorbate is desorbed, respectively. For a convenient solution for the calculation of PSD, Ac_j has to be replaced by the more general A_P. As, Ac_j is not constant, whereas the surface area of each pore,

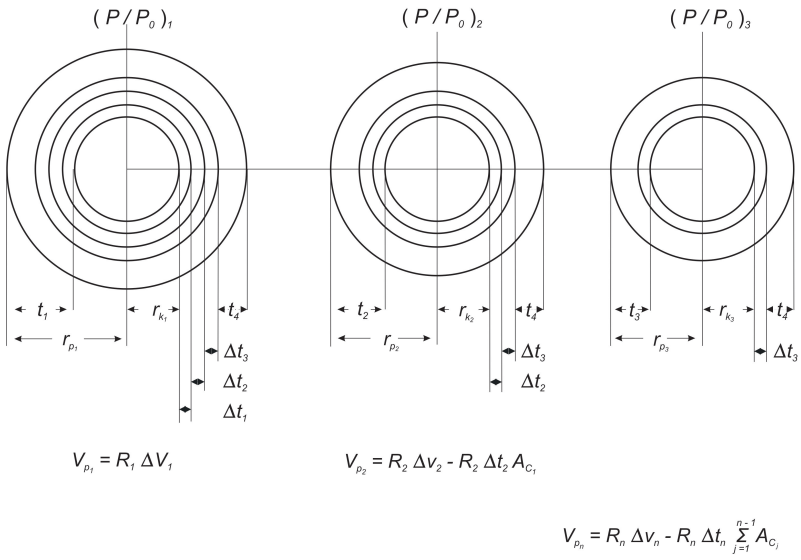

Figure 3.3: Desorption mechanism proposed by Barret, Joyner and Halenda for three pore diameters and for three steps in decreased pressure [266].

A_p, is constant. For an appropriate working function, a few more adjustments have to be made. One of these adjustments is to consider the proportion of $(\bar{r}_P - t_{\bar{r}})/\bar{r}_P$ to be a constant and mark it as c. In this expression, $\bar{r}_P$ and $\bar{t}_{\bar{r}}$ are the pore size emptied at the nth desorption step and the thickness of the physically adsorbed layer at the corresponding P/P_0. In reality, c varies as a function of $\bar{r}_p$. But in the case of a wide range of pores sizes, c can be considered constant. So, the final form of the equation is

$$V_{pn} = R_n \Delta V_n - R_n c \Delta t_n \sum_{j=1}^{n-1} A_{Pj}. \tag{3.8}$$

This equation can be used to determine the PSD for a material. The first term follows the equation 3.6 and defines the volume change of the inner capillary volume. The second term defines the area of the pores, which have not yet been emptied from condensate by a pressure decrease [266, 267].

Since the introduction of the BJH method, some new mathematical models have been developed to estimate PSD [268–272]. Horváth-Kawazoe introduced the thermodynamic approach for calculating PSD by applying the Gibbs function for adsorption. This model is especially applicable for mi-

croporous substances [269]. Another model that is widely used to determine PSD is the density functional theory (DFT) [273]. DFT is based on modern statistical mechanics [274] and is widely used in physics and chemistry in various modelling applications especially in atomic simulations [275–277]. With DFT, a basic integral for solving pore size distribution (PSD) can expressed as

$$N(P) = \int_0^\infty dH f(H)\rho(P, H) \tag{3.9}$$

where $N(P)$ stands for the number of moles adsorbed at the pressure P (measured isotherm), $\rho(P, H)$ is the theoretical uptake of nitrogen in a slit pore with a width of H at the pressure P and $f(H)$ is the function describing the pore size distribution [270, 274]. For this integral to be sufficient for determining PSD an appropriate individual pore isotherm $\rho(p, H)$ needs to be found [274]. Naturally, this causes a problem if this pore isotherm is not known. In addition, due to a heavy theoretical framework and inaccuracy, in some cases, DFT has not surpassed BJH as a standard method for determining PSD [278, 279]. Fig 3.4 shows the PSD from the same thermally-carbonized porous silicon sample using three different types of calculations. A simple calculation has been made by substituting relative pressure with the corresponding Kelvin radius and the adsorbed volume (y-axis) is presented with the corresponding length of the pores. The simple method in this case gives a pore radius that is slightly too large, because it is determined from the adsorption branch (red line in figure). Even though there are noticeable differences in the graphs, the distributions are quite consistent.

Models for measuring PSD have always been under scrutiny due to the fact that various assumptions have to be made for a mathematical model. Some characteristics pitfalls when determining PSD by conventional methods have been presented recently [273, 279, 280]. One fundamental issue is that BJH and many other methods are based on the Kelvin equation (3.4), which has some known limitations considering smaller mesopores [278, 280]. Though BJH has its limitations, it is a widely accepted algorithm for calculating PSD, as important factors are known and discrepancies of the model have been published[278]. For the most reliable calculations for PSD, one should always compare different algorithms to obtain the most accurate distribution [278].

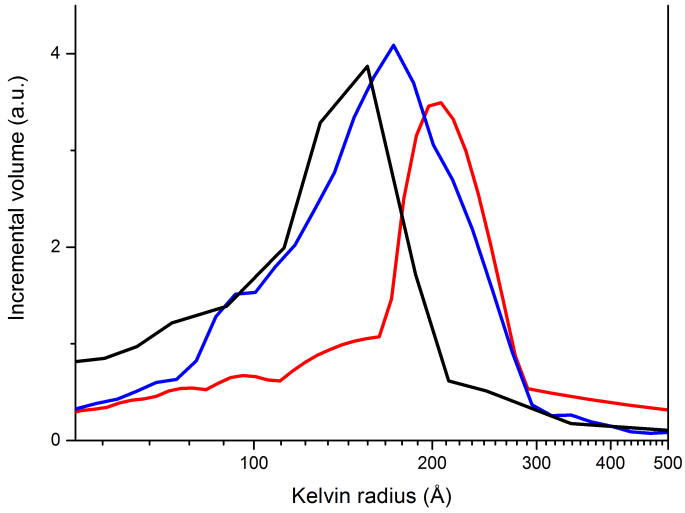

Figure 3.4: Pore size distributions determined by simple (red), BJH (black) and DFT (blue) methods. The Simple PSD has been determined from the adsorption isotherm, the others have been calculated from the desorption branch.

3.4 Humidity sensing

3.4.1 Humidity and hygroscopicity of a porous material

Excess water vapour, humidity, in the air constitutes many parasitic phenomena in industry. This means that ambient conditions need to be monitored for maintaining desired conditions.

Humidity can be described as the water vapour content of the atmosphere. At a given temperature only a certain amount of water can be in the gaseous phase, as vapour [252]. Pressure induced by vapour is also limited and this limit is called the saturated vapour pressure. Humidity is commonly expressed as a relative humidity ϕ, which is the relation of the prevailing P and the saturation P_0 vapour pressure

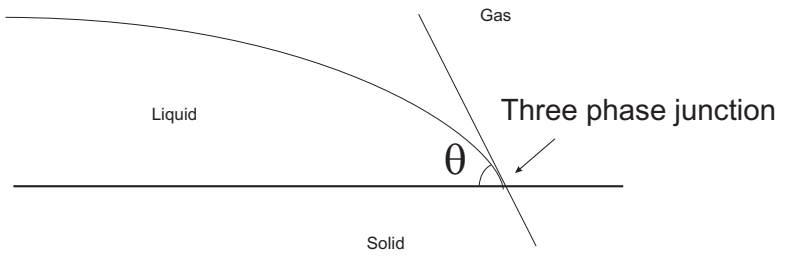

Figure 3.5: The contact angle of the liquid is determined from the three-phase junction. The contact angle θ has a significant role on the condensation of water into the pores in a porous media.

$$\phi = \frac{P}{P_0} \times 100\% \tag{3.10}$$

For the purpose of porous humidity sensors we present the Kelvin equation 3.4 as:

$$r = -\frac{2\gamma\bar{V}}{RT \ln \frac{P}{P_0}} cos\theta. \tag{3.11}$$

This form gives the pore radius r that is filled with condensed water. As can be seen from the equation 3.11, the pores with the radius r are filled according to the relative pressure $\frac{P}{P_0}$, temperature T and contact angle γ. The molar volume $\bar{V} = 18.1$ cm^3/mol and the surface tension of water $\gamma = 73$ N/m can be considered as constants.

Hygroscopicity is determined by the contact angle of water with a surface, at a constant temperature. Contact angle is measured from a three phase junction (see 3.5), when θ is near 0° the substance is considered to be hydrophilic and θ around 90° and above are hydrophobic surfaces. Superhydrophobic materials commonly have contact angles larger than 130 ° values [252].

Naturally, the temperature and size of the pores have their own effect on adsorption, but still the contact angle can be considered the most important feature for hygroscopicity.

3.4.2 Humidity sensors

Absolute humidity sensors

Absolute sensors comprise a few of the landmark techniques for detecting humidity and therefore they are used for the calibration of other humidity sensors. Absolute humidity sensors can be categorized into saturation and absorption [281, 282].

Dew point sensors are one of the most precise ways of detecting absolute humidity. They have a wide range too, so they are ideal for calibrating other humidity sensors. A dew point sensor is based on saturation, or more accurately vapor condensation, on a surface. Condensation can then be determined by either an optical, thermal or capacitive method. The condensation is achieved by cooling the detection surface with a thermoelectric device. According to the observed condensation at T_0 with the ambient temperature of T, the absolute humidity content can be calculated. Recently, industrial dew point sensors have changed to a more rugged construction, where a porous polymer is used as a sensitive sheet and the impedance of the sheet is monitored [281].

A wet and dry bulb psychrometer is one the most influential techniques for measuring humidity. While it lacks the precision of a dew point sensor, it still is more accurate than most humidity sensors. Its flaws are continuous maintenance and that it is somewhat onerous to operate. The working principle is extremely simple, a drop in temperature due to evaporation in a wet bulb. In a psychrometer, a thermometer in a dry bulb shows the ambient temperature, whereas a thermometer in a wet bulb has a lower temperature, which is proportionate to the evaporation speed of water from the bulb [281, 282].

A coulometer is an example of an absorption technique. In this humidity sensor, vapour is absorbed by a phosphorus pentaoxide (C_2P_5) layer. An electric field is applied through this layer to enable the electrolysis of water. By Faraday's law one can determine the current passing through the layer and the corresponding humidity. A coulometer is suitable for only part per billion (ppb) measurements, also it has long a response time [281].

Relative humidity sensors

Relative humidity measurements are divided into three categories: hygroscopic, spectral and other methods. Categorizing these methods into three

different types is vague, as all of them can be related more or less to hygroscopic methods.

Hygroscopic sensors react to humidity by changing their dimensions, mass or electrical characteristics. The largest category in this group of sensors is hygroscopic sensors and especially ones that change their electrical characteristics due water adsorption [281]. Usually the impedance of the hygroscopic layer is measured and there are numerous different technical designs for these sensors [281, 283–285]. One of the main reason impedance humidity sensors are popular is their easy and relatively cheap production combined with reasonable accuracy in detection [281]. Most of the sensors made from porous silicon fall into this category. The sensitivity of these types of sensors is commonly described for a certain humidity range by dividing the obtained difference of signals by the signal of the lower humidity (C_{max} - C_{min})/ C_{min} x 100%.

In spectral methods a characteristic absorption wavelength of water is observed with either ultraviolet or infrared instrumentation. For these methods the calibration for absorption has to be known to produce an accurate level of the relative humidity. The best practice for a spectral method is therefore to rather measure changes in humidity levels than the actual relative humidity.

Other methods consist of many different types of measurement systems, which could be included into the hygroscopic category assuming a loose definition for a hygroscopic material. Like the piezoelectric method, where a quartz crystal is coated with a hygroscopic material and the resonance frequency of the crystal will change according to the mass change of the coating material [281, 286]. One new method is to apply MEMS (Microelectromechanical systems) as a sensor material [287]. In MEMS sensors the adsorbtion of water on a cantilever or similar structure can be detected from *ie.* a change in the resonance frequency or a change in the position [286]. A brief summary of the humidity sensing techniques is shown in table 3.1.

3.4.3 Porous silicon humidity sensors

Humidity sensors made out of porous silicon can be considered as hygroscopic sensors, as the main principle for sensors is that water molecules are adsorbed onto the material. Due to a large surface area, this adsorption has a significant effect on the characteristics of PSi. Most of the sensor applications arise from a difference between the dielectric constant of PSi and water. A change in the apparent dielectric constant constitutes for a shift in the observed re-

Table 3.1: Categories of humidity sensors

Absolute humidity detection		
Operating principle	Description of typical instrumentation	Characteristics References
Saturation - Evaporation - Condensation	Dew point sensor, which is based on the condensation of water at certain temperatures Pshycrometer with dry and wet bulbs, which is based on the equilibrium of evaporation and temperature related to the evaporation rate	For standardization [156, 286, 288]
Absorption - Electrolysis	Coulometer Absorbed water is decomposed by an electric field, the current obtained from the electrolysis correlates the water content	Low RH only [289]
Relative humidity detection		
Hygroscopic - Impedance - Mass - Dimensions	Polar water molecules change the electrical characteristics Water changing conductance in material, The Dunmore sensor Impedance type sensors, where either capacitance or resistivity is changed due to water adsorption	Several technical approaches [156, 290, 291]
Spectral - Ultraviolet - Infrared	Absorption of characteristic wavelengths and abatement of intensity relative to the water content in the air Can detect several components from ambient conditions and is suitable for even volatile environments	Measures changes rather than the precise level of humidity [292]
Other - Piezoelectric - Refractive index - MEMS	Change in oscillation frequency due to the adsorption of water Change in the refractive index due to condensed water, especially in porous reflectors	Numerous approaches [156, 286, 287, 292–294]

fractive index and impedance, this translates into the detected species as: conductivity, resistivity, capacitance, reflectance spectrum, etc. The use of PSi as an optical sensor has been presented in ref [151] in detail. A short summary of the different kinds of gas and humidity sensors made from PSi can be found in table 3.2.

The sensitivity of PSi sensors, combined with existing silicon-based technologies, gives them a clear advantage over commercially available sensors. In addition, poor detection accuracy and slow response times are common deficiencies in moderately priced commercial sensors. On the other hand, significant hysteresis and the lack of chemical stability in PSi sensors have been seen as severe drawbacks for the commercial utilization of PSi sensors so far. Although there are no clear definitions for good stability or reasonable sensitivity, there are some desired values for commercial sensors, like a stability change below 1Impedance in PSi sensors is composed of the capacitive reactance (X_C) and resistivity (R). Of these, the capacitive reactance or more precisely capacitance is used for sensing purposes [10]. The capacitance of a simple plate capacitor is in the form of

$$C = \frac{\varepsilon_0 \varepsilon_m A}{d}, \tag{3.12}$$

where ε_0 is the permittivity of free space and ε_m is the apparent permittivity of silicon and water. A is the area of the capacitor and d is the distance of the capacitor plates. The apparent permittivity can be estimated by a traditional effective media approximation like the Bruggeman equation [295]

$$\sum_{i=1}^{n_c} f_i \frac{\varepsilon_i - \varepsilon}{\varepsilon_i + 2\varepsilon} = 0. \tag{3.13}$$

Where f_i is the volume fraction of a particular component. In this equation ε stands for the effective permittivity for the entire system. For silicon and water the equation can be written as

$$f_{Si} \frac{\varepsilon_{Si} - \varepsilon}{\varepsilon_{Si} + 2\varepsilon} + f_w \frac{\varepsilon_w - \varepsilon}{\varepsilon_w + 2\varepsilon} = 0. \tag{3.14}$$

In the case of porous Si, during water adsorption only f_w can be considered as a variable in this equation. The water content can be estimated by the Kelvin equation 3.4 for a known pore size distribution. When considering the exact composition of a capacitor made of PSi, the surface effect of

SiO_x (ε_{SiO_x} =3.9) and SiC ($\varepsilon_{SiC} = 6.5 - 9.7$)can be significant, for pure Si $\varepsilon_{Si} = 11.68$ and for water $\varepsilon_w = 80$ [296].

Typically PSi sensors are made on a substrate, which changes the structure into two parallel capacitors and the actual capacitance is

$$C = C_1 + C_2 = \frac{\varepsilon_0 \varepsilon_{Si} A_{Si}}{d_{Si}} + \frac{\varepsilon_0 \varepsilon_{Si+w} A_{Si+w}}{d_{Si+w}}. \tag{3.15}$$

In this equation, the first term remains constant and only the latter part changes according to the proportion of the water filling the pores. For porous humidity sensors it is known that at low humidity levels, proton hopping between adsorption sites is responsible for conductivity and when water forms multilayers or condensates, the Grotthuss chain reaction starts to dominate within porous media [281, 297]. This complicates the situation of modelling the performance of PSi sensors. Moreover, the uneven pore size distribution has a distinctive effect on the response of the sensor and also the surface chemistry of the sensor might obscure the obtained capacitance.

Table 3.2: Summary of different sensors based on porous silicon. Optical sensors are dependent on changes in the refractive index except photoluminescent sensors. In the case of electrical sensors, conductivity is the main parameter to be detected and only capacitor type sensors are based on changes in the dielectric constant [285]

Optical sensors		
Architecture	Sensed quantity Sensed property	References
Single layer	Photoluminescence intensity or spectrum	[134, 137, 138, 138, 139, 298]
Single layer	Reflectance spectrum Intensity of spectrum	[299–301]
Waveguide	Transmission losses Intensity of spectrum	[302]
Bragg	Reflectance spectrum Intensity of spectrum	[147, 303, 304]
Resonant cavity	Resonance peak position Wavelength	[305, 306]
Rugate filter	Reflectance peak position Wavelength	[143, 189, 307]
Electrical sensors		
Capacitor	Capacitance Dielectric constant	[10, 136, 308–311]
Schottky-like diode	Current Energy barrier	[59, 312]
Resistor	Resistance Conductivity	[58, 313–315]
FET-like transistor	Impedance Dielectric constant	[316, 317]
Junction-like diode	Current Energy barrier	[318]

Chapter 4

Aims of the study

The foundations of the present study have been cemented in previous years by PhD Salonen and PhD Björkqvist in the Laboratory of Industrial Physics [140, 141, 235, 310, 319]. They have studied and developed fabrication procedures for thermally-carbonized porous silicon (TCPSi) as well as for humidity sensors. Some of the procedures are well-established practices nowadays used in the production of TCPSi-based humidity and gas sensors. Nevertheless, some new techniques were developed during this study.

In this thesis, efforts have been made to further enhance the properties of the TCPSi humidity sensors. Especially, the reduction of hysteresis has been a major part of the study. In addition, stability issues have been considered. Another major object of this study was to find ways to enhance the sensitivity of the sensor.

Hysteresis is seen in mesoporous structures during gas sorption processes (Paper I). For porous gas sensors, it leads to reliability problems especially, if the partial pressure of the gas decreases. A typical method for cancelling out this problem is to heat up the sensor for variable lengths of time. In the case of TCPSi, several manufacturing methods can be used to overcome this problem. The hygroscopicity of the surface of TCPSi can be adjusted by the processing temperature of the acetylene treatment (Paper I). Varying the processing temperature and acetylene flow during the process, one can obtain either a hydrophobic or hydrophilic surface. Naturally, the average pore diameter of the TCPSi has an effect on hysteresis as well, but it can also be adjusted with numerous different methods. In the case of TCPSi, we have used annealing of the samples in a nitrogen atmosphere (Paper II). In

this study, the three methods mentioned above were studied to find the most feasible way to reduce hysteresis in TCPSi humidity sensors.

Stability issues are always presented in the context of PSi. The long term stability of the TCPSi humidity sensor was studied also as a part of this research (Paper III).

The main part of the present study was to achieve better sensitivity of the sensor with significantly reduced hysteresis. Overall, electrical isolation of the sensing layer was evaluated to be the most prominent way to enhance the characteristics of the TCPSi sensor (Paper IV). With electrical isolation, bypassing of the current via the substrate is inhibited. In the case of TCPSi, a new layer can be etched underneath and therefore an electrical isolation layer can be produced. Oxidation was chosen to create electrical isolation of the TCPSi sensing layer, as oxidized PSi is a common electrical isolation in semiconductor production and has proved its quality as an insulation material. Thermal oxidation was omitted from the studies, as temperatures above 300 °C are detrimental for the electrical properties of a thermally-carbonized surface. Both chemical and electrochemical oxidation methods were utilized to find a suitable way of oxidizing the isolation layer.

Chapter 5

Experimental

5.1 Electrical measurements

In previous studies [141, 310] TCPSi humidity sensors were found to function as capacitive sensors, as their resistivity is extremely sensitive to changes in temperature [319, 320]. This results in varying resistivity in TCPSi, which is not related to the relative humidity change, but to heat transfer during adsorption and desorption [321].

Electrical measurements were performed with a Quadtehch 1920 Precision LCR meter. According to previous studies, the capacitance is dependent on the frequency. Furthermore, 120 Hz has been found to be an ideal frequency, with the best noise to signal ratio in normal RH atmosphere measurements. However, changes in capacitance during storage were also monitored with several frequencies, Paper III.

5.2 Hygroscopicity measurements

5.2.1 Contact angle measurements

The contact angle can be measured with various methods. Sessile drop or captive bubble methods are the most common ways to determine the contact angle of the liquid - surface interface. The contact angle in these methods can be calculated from the equation

$$\tan\frac{\theta}{2} = \frac{h}{r} \tag{5.1}$$

where h and r are the height and radius of the droplet [252]. Nowadays, the contact angle is measured automatically by the analysing program from the three-phase junction, see figure 3.5. In this study the Dynamic adsorption tester DAT 1100 (Fibro system) was used to measure the contact angle of fresh, oxidized and thermally-carbonized PSi samples.

5.2.2 Hygroscopicity measurement apparatus

A hygroscopicity measurements apparatus (HMA) is a gravimetric device, which measures the quantity of the adsorbed water into a medium. Water is adsorbed from the atmosphere and the humidity of the atmosphere is controlled by saturated salt solutions.

The idea of the HMA is extremely simple, one just weighs the mass of the material in different relative humidities. Data from the HMA is bound to the relative humidities of the saturated salt solutions, but one can select suitable salt solutions for almost any purpose.

.

5.2.3 Isothermal microcalorimetry

Like HMA, isothermal microcalorimetry (IMC) is based on a rather simple principle. IMC measures any heat transferring from or to a sample in a test chamber. This is compared to an empty reference chamber, so that the difference in heat flow between the reference and sample chambers is detected. Due to the principle of the method, IMC data is unspecified, so that IMC measurements usually need some additional methods for obtaining information about the processes to be studied in the sample.

Any specific reaction is dissipated under the overall heat transfer, and normally X-ray diffraction and infra-red spectroscopy are suitable techniques for constructing reaction kinematics between starting substances and the final product. For the water adsorption studies presented in papers I and II, the HMA and contact angle measurements were suitable methods to accompany IMC measurements.

5.3 Gas sorption measurements

In this study, a Tristar 3000 (Micromeritics) was used for gas sorption measurements. BJH, BET and DFT analyses were performed for the porous silicon samples. BET and BJH were used for determining the surface area of the samples. DFT was mainly used for analysing the pore size distribution of the samples. The idea behind the mathematical interpretation of specific surface areas and pore size distributions is presented in chapter 3.

The principle of the actual measurement is the following. The sample is placed into a vessel with a known volume. At first, there is a vacuum inside the vessel. After a sufficient level of vacuum is reached, the inert gas is lead into the vessel. The pressure of the inert gas is measured before dosing. As the gas is adsorbed on the surface of the sample, the pressure inside the vessel diminishes. At equilibrium, the pressure reaches a certain value and when compared to the original pressure value, which would be obtained without a sample, the difference gives the amount of the adsorbed gas. So, only the value of the gas pressure has to be known. This can be done several times until the saturation pressure of the gas is reached. Every time the pressure of the dosed gas and the prevailing pressure at equilibrium are collected. From this data, one can draw the isotherm of the volume adsorbed or absorbed by the sample in various relative pressures and furthermore apply BET, BJH and DFT analyses to estimate the characteristics of the PSi.

Chapter 6

Results and discussion of papers

6.1 Paper I

In this study, the hygroscopicity of the TCPSi was determined by means of contact angle and sorption measurements. Hygroscopicity or hydrophobicity was seen as a possible method for reducing hysteresis in TCPSi sensors, as the hydrophopicity can be tuned in TCPSi. As is presented in the paper, the hydrophobicity is dependent on the processing temperature of the acetylene treatment and also on whether the acetylene flush is used during the thermal treatment. The contact angle can be used to estimate the pore filling due to adsorption at different relative humidities according to the Kelvin equation. The energy of sorption was determined by isothermal microcalorimetry (IMC) and the mass of the adsorbed water was determined by a hycroscopicity measurement apparatus (HMA). When IMC and HMA data are combined, the energy of adsorption can be calculated.

According to the study, the tuning of the contact angle is an effective way of reducing the hysteresis in TCPSi. Tuning of the contact angle is based on the hydrogen content on a surface of the pores. Hydrogen desorption during a heat treatment of the thermal carbonization can be compensated for by an acetylene flow. Samples which had been exposed to an acetylene flow during the heat treatment showed contact angles above 80°, whereas samples under similar treatment conditions without an acetylene flow had contact angles of about 30°. A strong indication for hydrogen desorption

during a heat treatment can be assumed from the sample, which was exposed to the acetylene flow for only half of the treatment time. This sample had a contact angle clearly smaller than did the sample with the acetylene flow, but a considerably larger angle than the sample without the acetylene flow.

The Kelvin equation describes the condensation on porous media. Assuming room temperature and water as an adsorbate, there is only one parameter in the equation, the contact angle. The effect of the contact angle becomes notable when comparing the condensation curve with a contact angle of 25° and 71° (Fig. 6.1). Only a small portion of the pores have been filled with condensed water at RH 85%, namely those with a diameter below 4.2 nm, in a sample with = 71°. In contrast, a hydrophilic sample with = 25° has already all of its pores up to 10 nm filled at RH 85%, which means that a majority of the pores has a condensed water content. Actually, this is visible also in HMA measurements. Samples with a low contact angle demonstarted a weight increase of about 40% and the mass change was immeasurable when the angle was close to 90°.

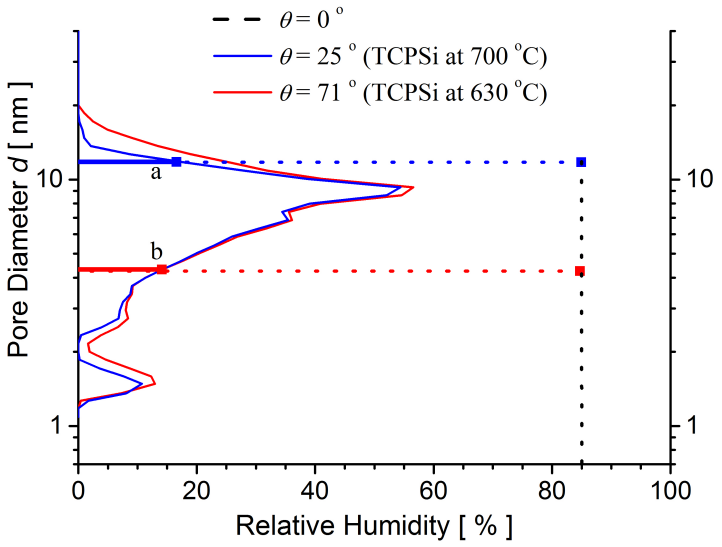

Figure 6.1: Kelvin diameter of the pores and the effect of the contact angle on pore filling at different relative humidities. Pore size distributions for TCPSi samples are shown on the left vertical axis.

Naturally, hysteresis is strong in hydrophilic samples with a PSD shown in Fig. 6.2. Recorded hystereses have been more than 50% at RH 85% when decreased from 95% for samples with less than 30°, whereas for hydrophobic samples the hysteresis was negligible.

A few outcomes of this paper should be mentioned: Adsorption on hydrophilic samples had one interesting feature, which was briefly mentioned in the paper. This is the observation, that the adsorption energy drops below the bulk adsorption energy of water when adsorbed by TCPSi. Also, the possibility of accurately adjusting the contact angle of water will also enable the control of hysteresis.

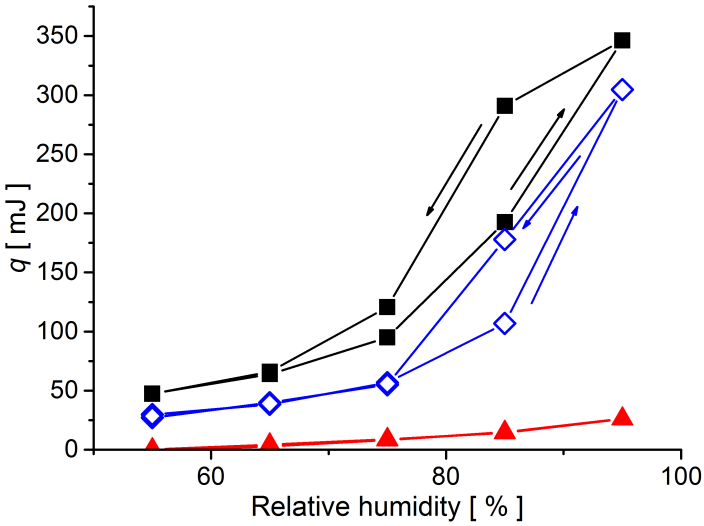

Figure 6.2: Hysteresis detected from the heat of sorption for three different thermal carbonizations. For the hydrophobic surface, the heat of sorption is negligible.

6.2 Paper II

The applications for reducing hysteresis in TCPSi sensors are discussed in paper II. Three different methods for reducing hysteresis and their possible suitability and disadvantages were studied. As an extension from paper I

the hygroscopicity of the TCPSi in the sensors was studied. Also, the heating of the TCPSi sensor during humidity detection as well as the pore size enlargement of the pores in TCPSi sensors by annealing were explored.

The measurements in this study concentrated on the testing of sensors with different process procedures to optimize hysteresis. Tests were done in a gas line where dry synthetic air was mixed with humidified synthetic air, which was obtained by directing air into a bubbling chamber. By controlling the volumetric proportion of the dry and humid air, the eligible relative humidities were achieved.

Modification of the contact angle between the pore surface and water presented anomalies that inhibited the use of such a treatment for sensor production. Instead, both pore size enlargement and heating of the sensor were found suitable for minimizing hysteresis in sensors. However, eventually pore size enlargement was chosen for sensor studies, as it is simple to use in sensor production.

Hysteresis diminished with pore size enlargement, but this resulted in a decrease in pore surface area, which came down from 280 cm^2 /g to 70 cm^2/g. This also meant that the sensitivity of the sensors was decreased. Similar behaviour was seen in heated sensors. In contrast to pore size enlargement, heating results in lower levels of condensed water inside the pores, even when the temperature of the sensor is raised only by a few degrees above ambient temperature. The thermistor behaviour of the TCPSi enables the precise monitoring of the temperature of the sensor, and thereby an accurate relative humidity measurement can be achieved.

During this study, the consistency in the production of the TCPSi was placed under scrutiny. Also, sensitivity issues became a concern, as the reduction in hysteresis also decreased sensitivity, because pore enlargement was determined to be the best way of reducing hysteresis.

6.3 Paper III

In this study, the long-term effects of ageing on a TCPSi humidity sensor were determined. Like in paper II, this study focused on the performance of the TCPSi sensor. However, in this case the production procedure was already determined in a previous study.

There were a few interesting features that became apparent during the ageing process. Not only was the ageing rapid in the first month of operating

the sensor, but also the way the ageing affected the sensor was quite interesting. As is shown in Fig. 6.3, the capacitance increases at low humidities and decreases at high humidities, so that the overall drop in sensitivity is significant. After the first few months, the capacitance values stabilize for respective RH values. This is a quite commonly observed phenomenon and usually it can be solved by the rapid pre-aging of the sensor.

Nevertheless, after one year of operating the sensor the capacitance values started to equally decrease. Still, the sensitivity of the sensor remained the same. The ageing of the sensor showed also one very interesting feature. This was observed when the capacitance was measured at different frequencies. The study provided proof that frequencies below 1 kHz are adequate for detecting humidity. Hence, the normally used frequency of 120 Hz is applicable for this purpose. In Fig. 6.4 the capacitance values of the sensor as a function of frequency are shown. Measurements were done after 211 and 311 days of storage, so that the sensor was already well aged. The capacitance values are in correspondence with the applied humidity for both cases when the frequency is below 1 kHz. With frequencies above 1 kHz, the capacitance values seem to correspondent with the age of the sensor only.

The conclusions of this study were that, even though the TCPSi sensor does exhibit changes in performance in the long-term, the operation is quite consistent and this study also proved that using a frequency of 120 Hz is suitable for sensing humidity. Frequencies above 1 kHz are unsuitable for humidity detection in the long run, but may be useful when internal recalibration methods are considered.

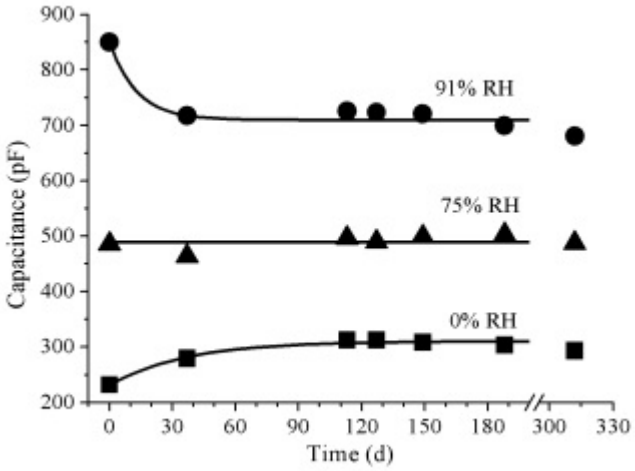

Figure 6.3: Capacitance values of the sensor measured during long-term storage. The decrease in capacitance on high RH and increase on low RH, results in diminished sensitivity.

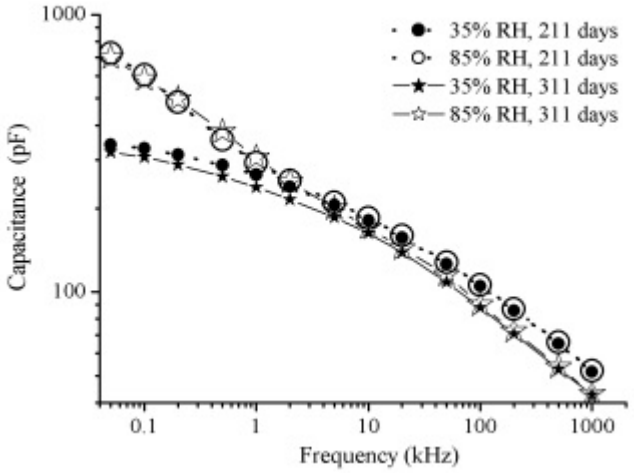

Figure 6.4: Capacitance measured after storage with several frequencies. the high and low humidities are separated at lower than 1 kHz frequencies, whereas above this frequency level no distinction can be made between low or high humidity.

6.4 Paper IV

This study was based on the idea that sensitivity is attenuated by the current bypassing via a substrate during measurements. Hence, the electrical isolation of the porous silicon layer or the sensing layer would be an ideal approach for increasing the sensitivity of the sensor, which was decreased due to the annealing process described in the previous papers. Electrical isolation is conceivable for the TCPSi sensing layer as it is resistant against HF and therefore a new layer can be etched underneath the TCPSi layer.

Three different oxidation methods were used to obtain electrical isolation underneath the TCPSi sensing layer. Thermal oxidation was omitted as it was already shown that TCPSi is vulnerable to thermal oxidation [235]. Two pyridine assisted oxidation methods and electrical oxidation were used, liquid and vapor oxidation. Pyridine assisted oxidation is extremely violent for Psi, but in the case of TCPSi, only slight oxidation was observed according to changes in pore size distribution (Fig. 6.5 and 6.6). On the other hand, the TCPSi - PSi interface suffers from the strong oxidation of Psi, and TCPSi is somewhat detached from the underlying surface. Therefore, pyridine assisted oxidation was also omitted. Electrochemical oxidation on the other hand has a notable effect on the pore size distribution in TCPSi. However, the actual distribution seems to be same, but it was shifted towards smaller pores (Fig. 6.7). Electrochemical oxidation caused a smooth transition from the oxide to a thermally-carbonized layer and therefore this method was chosen for the electrical isolation of the sensor structure.

Testing of the TCPSi sensors with electrical isolation of the sensing layer (EISL) showed that the sensitivity of the sensor was remarkably better compared to previously used TCPSi sensors and still retained the fast response time for rapid changes in humidity.

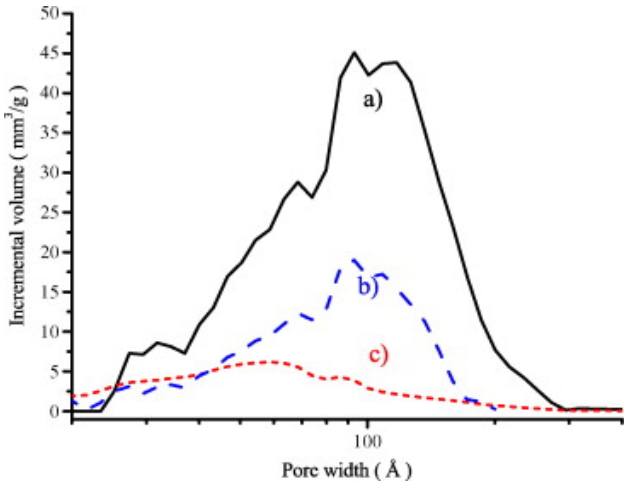

Figure 6.5: Incremental volume vs. pore width of (a) original PSD, (b) PSD of the PSi layer after electrochemical oxidation and (c) PSD of the PSi layer after pyridine assisted liquid oxidation.

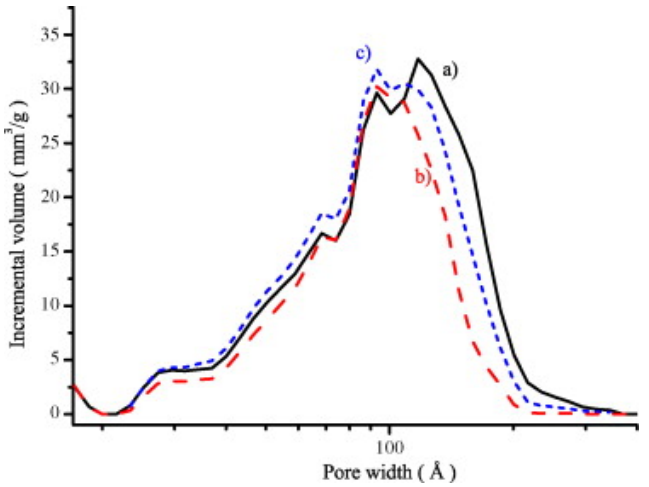

Figure 6.6: Effects of the pyridine-assisted oxidations on the pores of the TCPSi; (a) original PSD, (b) PSD after vapor and (c) liquid oxidation with pyridine.

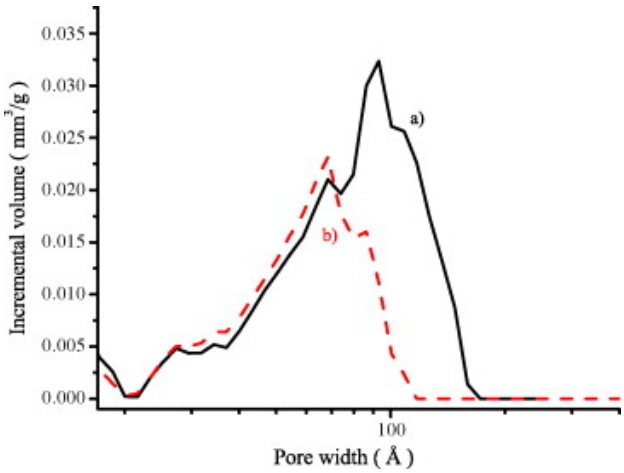

Figure 6.7: The pore sizes and corresponding volumes diminish evenly for all pores, when TCPSi is electrochemically oxidized.

Chapter 7

Conclusions

In the present study, the aim was to find parameters for the optimization of the TCPSi humidity sensor. In the first part, the surface chemistry and pore size depedency of the hysteresis were studied, and an appropriate way of manufacturing the TCPSi sensor was found. Modification of the contact angle resulted in anomalies in the sensor response for surface chemistries with low hygroscopicity. The most effective way to reduce hysteresis was found to be annealing of the PSi before thermal carbonization. Also, slight heating of the sensor was effective. In both cases the sensitivity of the sensor was reduced as a consequence of the lower surface area of the pores or lower amount of condensed water inside the pores.

The second part of the study focused on stability issues of the TCPSi. For this part of the study a new, more effective carbonization process was adopted. The results show that the sensitivity of the TCPSi sensor was considerably more stable after 60 days to up to 312 days. The decrease during the first 60 days were assigned to changes in electrical contacts and slight oxidation of the TCPSi surface. The capacitance of the sensor with different frequencies were found to be solely related to age of the sample with test frequencies above 1 kHz. So, reliable humidity detection is perceived at frequencies under 1 kHz.

As was mentioned before, the sensitivity decreased when hysteresis was reduced to an appropriate level. So in the last part of the study, a method for increasing sensitivity was developed. Electrical isolation of the sensing layer was considered a solution for this problem. As TCPSi is resistant towards HF, this enables the consecutive etching of the layer beneath the TCPSi layer. It is possible to oxidise this new layer because TCPSi is inert enough

towards most corrosives. An electrically isolated sensing layer (EISL) for sensing purposes was introduced based on the TCPSi humidity sensor. The sensitivity of this sensor was significantly enhanced by EISL compared to a typical TCPSi sensor.

The TCPSi humidity sensor has already shown good reproducibility and reasonable sensitivity. In this thesis some of the parameters were optimized for sensing purposes. Hysteresis of the porous sensor was decreased by enlargement of the pores and the resulting decrease in sensitivity was restored and even enhanced with an EISL structure. The research also added to our understanding of TCPSi, and an advanced thermal treatment was applied in the production of TCPSi. The temperature dependency of the EISL TCPSi sensor enables the use of the sensor as a temperature probe as well, and in future an integrated humidity and temperature sensor should be pursued. Also, new multilayer structures with several different surface chemistries should be studied more closely.

Bibliography

[1] D. R. Turner, "Electropolishing Silicon In Hydrofluoric Acid Solutions," *J. Electrochem. Soc.*, vol. 105, pp. 402–408, 1958.

[2] R. J. Archer, "Stain Films On Silicon," *J. Phys. Chem. Solids*, vol. 14, pp. 104–110, 1960.

[3] D. H. Everett, ed., *Manual of Symbols and Terminology for Physicochemical Quantaties and Units*. Butterworths, London, 1972.

[4] V. Lehmann, "The Physics of Macropore Formation In Low Doped N-type Silicon," *J. Electrochem. Soc.*, vol. 140, pp. 2836–2843, 1993.

[5] V. Lehmann and U. Grüning, "The limits of macropore array fabrication," *Thin Solid Films*, vol. 297, pp. 13–17, 1997.

[6] H. Föll, M. Christophersen, J. Carstensen, and G. Hasse, "Formation and application of porous silicon," *Mater. Sci. Eng. R Reports*, vol. 39, pp. 93–141, 2002.

[7] H. Ouyang, M. Christophersen, R. Viard, B. L. Miller, and P. M. Fauchet, "Macroporous Silicon Microcavities for Macromolecule Detection," *Adv. Funct. Mater.*, vol. 15, pp. 1851–1859, 2005.

[8] K. Kobayashi, F. A. Harraz, S. Izuo, T. Sakka, and Y. H. Ogata, "Macropore growth in a prepatterned p-type silicon wafer," *Phys. status solidi*, vol. 204, pp. 1321–1326, 2007.

[9] O. Bisi, S. Ossicini, and L. Pavesi, "Porous silicon: a quantum sponge structure for silicon based optoelectronics," *Surf. Sci. Rep.*, vol. 38, pp. 1–126, 2000.

[10] R. C. Anderson, R. S. Muller, and C. W. Tobias, "Investigations of porous silicon for vapor sensing," *Sensors Actuators A Phys.*, vol. 23, pp. 835–839, 1990.

[11] J. Wagner, "Photoluminescence and excitation spectroscopy in heavily doped n - and p -type silicon," *Phys. Rev. B*, vol. 29, pp. 2002–2009, 1984.

[12] L. T. Canham, "Silicon Quantum Wire Array Fabrication By Electrochemical and Chemical Dissolution of Wafers," *Appl. Phys. Lett.*, vol. 57, pp. 1046–1048, 1990.

[13] V. Lehmann and U. Gösele, "Porous Silicon Formation - A Quantum Wire Effect," *Appl. Phys. Lett.*, vol. 58, pp. 856–858, 1991.

[14] A. Uhlir, "Electrolytic Shaping of Germanium and Silicon," *Bell Syst. Tech. J.*, vol. 35, pp. 333–347, 1956.

[15] Web of Knowledge, "Search topic: Infrared spectroscopy (Accessed 2009-10-15)."

[16] K. H. Beckmann, "Investigation of Chemical Properties of Stain Films On Silicon By Means of Infrared Spectroscopy," *Surf. Sci.*, vol. 3, pp. 314–332, 1965.

[17] R. Memming and G. Schwandt, "Anodic Dissolution of Silicon In Hydrofluoric Acid Solutions," *Surf. Sci.*, vol. 4, pp. 109–124, 1966.

[18] Y. Watanabe and T. Sakai, "Application of A Thick Anode Film To Semiconductor Devices," *Rev. Electr. Commun. Lab.*, vol. 19, pp. 899–903, 1971.

[19] Y. Watanabe, Y. Arita, T. Yokohama, and Y. Igarashi, "Novel Isolation Technique By Oxidation of Porous Silicon," *J. Electrochem. Soc.*, vol. 120, pp. C235–C235, 1973.

[20] Y. Watanabe, Y. Arita, T. Yokohama, and Y. Igarashi, "Formation and Properties of Porous Silicon and Its Application," *J. Electrochem. Soc.*, vol. 122, pp. 1351–1355, 1975.

[21] K. Imai, "A New Dielectric Isolation Method Using Porous Silicon," *Solid. State. Electron.*, vol. 24, pp. 159–164, 1981.

[22] G. Bomchil, A. Halimaoui, and R. Herino, "Porous Silicon - the Material and Its Applications In Silicon On Insulator Technologies," *Appl. Surf. Sci.*, vol. 41-42, pp. 604–613, 1989.

[23] Y. Arita, "Formation and Oxidation of Porous Silicon By Anodic Reaction," *J. Cryst. Growth*, vol. 45, pp. 383–392, 1978.

[24] T. Unagami, "Formation Mechanism of Porous Silicon Layer By Anodization In Hf Solution," *J. Electrochem. Soc.*, vol. 127, pp. 476–483, 1980.

[25] M. I. J. Beale, N. G. Chew, M. J. Uren, A. G. Cullis, and J. D. Benjamin, "Microstructure and Formation Mechanism of Porous Silicon," *Appl. Phys. Lett.*, vol. 46, pp. 86–88, 1985.

[26] M. I. J. Beale, J. D. Benjamin, M. J. Uren, N. G. Chew, and A. G. Cullis, "An Experimental and Theoretical-study of the Formation and Microstructure of Porous Silicon," *J. Cryst. Growth*, vol. 73, pp. 622–636, 1985.

[27] T. Unagami and M. Seki, "Structure of Porous Silicon Layer and Heat-treatment Effect," *J. Electrochem. Soc.*, vol. 125, pp. 1339–1344, 1978.

[28] G. Bomchil, R. Herino, K. Barla, and J. C. Pfister, "Pore-size Distribution In Porous Silicon Studied By Adsorption-isotherms," *J. Electrochem. Soc.*, vol. 130, pp. 1611–1614, 1983.

[29] C. Pickering, M. I. J. Beale, D. J. Robbins, P. J. Pearson, and R. Greef, "Optical Studies of the Structure of Porous Silicon Films Formed In P-type Degenerate and Non-degenerate Silicon," *J. Phys. C-solid State Phys.*, vol. 17, pp. 6535–6552, 1984.

[30] C. Pickering, M. I. J. Beale, D. J. Robbins, P. J. Pearson, and R. Greef, "Optical-properties of Porous Silicon Films," *Thin Solid Films*, vol. 125, pp. 157–163, 1985.

[31] R. Herino, G. Bomchil, K. Barla, C. Bertrand, and J. L. Ginoux, "Porosity and Pore-size Distributions of Porous Silicon Layers," *J. Electrochem. Soc.*, vol. 134, pp. 1994–2000, 1987.

[32] L. T. Canham, "Room-temperature Photoluminescence From Etched Silicon Surfaces - the Effects of Chemical Pretreatments and Gaseous Ambients," *J. Phys. Chem. Solids*, vol. 47, pp. 363–373, 1986.

[33] L. T. Canham, M. R. Dyball, W. Y. Leong, M. R. Houlton, A. G. Cullis, and P. W. Smith, "Radiative Recombination Channels Due To Hydrogen In Crystalline Silicon," *Mater. Sci. Eng. B-solid State Mater. Adv. Technol.*, vol. 4, pp. 41–45, 1989.

[34] N. Koshida and H. Koyama, "Efficient Visible Photoluminescence From Porous Silicon," *Japanese J. Appl. Phys. Part 2-letters*, vol. 30, pp. L1221—-L1223, 1991.

[35] A. Halimaoui, C. Oules, G. Bomchil, A. Bsiesy, F. Gaspard, R. Herino, M. Ligeon, and F. Muller, "Electroluminescence In the Visible Range During Anodic-oxidation of Porous Silicon Films," *Appl. Phys. Lett.*, vol. 59, pp. 304–306, 1991.

[36] P. McCord, S. L. Yau, and A. J. Bard, "Chemiluminescence of anodized and etched silicon: Evidence for a luminescent siloxene-like layer on porous silicon," *Science (80-.).*, vol. 257, pp. 68–69, 1992.

[37] L. T. Canham, W. Y. Leong, M. I. J. Beale, T. I. Cox, and L. Taylor, "Efficient Visible Electroluminescence From Highly Porous Silicon Under Cathodic Bias," *Appl. Phys. Lett.*, vol. 61, pp. 2563–2565, 1992.

[38] X. G. Zhang, "Mechanism of pore formation on n-type silicon," *J. Electrochem. Soc.*, vol. 138, pp. 3750–3756, 1991.

[39] R. L. Smith and S. D. Collins, "Porous Silicon Formation Mechanisms," *J. Appl. Phys.*, vol. 71, pp. R1—-R22, 1992.

[40] P. C. Searson, J. M. Macaulay, and S. M. Prokes, "Formation, morphology, and optical properties of porous silicon structures," *J. Electrochem. Soc.*, vol. 139, pp. 3373–3378, 1992.

[41] Y. Kang, "Morphological Stability Analysis of Porous Silicon Formation," *J. Electrochem. Soc.*, vol. 140, pp. 2258–2265, 1993.

[42] J. Erlebacher, P. Searson, and K. Sieradzki, "Computer simulations of dense-branching patterns," *Phys. Rev. Lett.*, vol. 71, pp. 3311–3314, nov 1993.

[43] G. John and V. Singh, "Diffusion-induced nucleation model for the formation of porous silicon," *Phys. Rev. B*, vol. 52, pp. 11125–11131, 1995.

[44] Z. He, Y. Huang, and R. Kwor, "A modified computer model for the formation of porous silicon," *Thin Solid Films*, vol. 265, pp. 96–100, 1995.

[45] S. Frohnhoff, "An Extended Quantum Model for Porous Silicon Formation," *J. Electrochem. Soc.*, vol. 142, pp. 615–620, 1995.

[46] R. M. Vadjikar, A. K. Nath, and A. N. Chandorkar, "Formation and growth of porous silicon," *Nanostructured Mater.*, vol. 8, pp. 507–520, 1997.

[47] Y. Kang, "Dissolution Mechanism for p-Si during Porous Silicon Formation," *J. Electrochem. Soc.*, vol. 144, pp. 3104–3111, 1997.

[48] E. S. Kooij, "Catalysis and Pore Initiation in the Anodic Dissolution of Silicon in HF," *J. Electrochem. Soc.*, vol. 144, pp. 1296–1301, 1997.

[49] J. Carstensen, R. Prange, G. Popkirov, and H. Föll, "A model for current oscillations in the Si-HF system based on a quantitative analysis of current transients," *Appl. Phys. A Mater. Sci. Process.*, vol. 67, pp. 459–467, 1998.

[50] L. N. Aleksandrov and P. L. Novikov, "Mechanisms of formation and topological analysis of porous silicon computational modeling," *Comput. Mater. Sci.*, vol. 10, pp. 406–410, 1998.

[51] J. Carstensen, "A Model for Current-Voltage Oscillations at the Silicon Electrode and Comparison with Experimental Results," *J. Electrochem. Soc.*, vol. 146, pp. 1134–1140, 1999.

[52] K. W. Kolasinski, "The mechanism of Si etching in fluoride solutions," *Phys. Chem. Chem. Phys.*, vol. 5, pp. 1270–1278, 2003.

[53] E. Foca, J. Carstensen, and H. Föll, "Modelling electrochemical current and potential oscillations at the Si electrode," *J. Electroanal. Chem.*, vol. 603, pp. 175–202, 2007.

[54] V. P. Parkhutik, J. M. Albella, J. M. MartinezDuart, J. M. GómezRodríguez, A. M. Baró, and V. I. Shershulsky, "Different types of pore structure in porous silicon," *Appl. Phys. Lett.*, vol. 62, pp. 366–368, 1993.

[55] V. Petrova-Koch, T. Muschik, A. Kux, B. K. Meyer, F. Koch, and V. Lehmann, "Rapid-thermal-oxidized porous Si-The superior photoluminescent Si," *Appl. Phys. Lett.*, vol. 61, pp. 943–945, 1992.

[56] A. Bsiesy, J. C. Vial, F. Gaspard, R. Herino, M. Ligeon, F. Muller, R. Romestain, A. Wasiela, A. Halimaoui, and G. Bomchil, "Photoluminescence of High Porosity and of Electrochemically Oxidized Porous Silicon Layers," *Surf. Sci.*, vol. 254, pp. 195–200, 1991.

[57] T. Taliercio, M. Dilhan, E. Massone, A. Gué, B. Fraisse, and A. Foucaran, "Realization of porous silicon membranes for gas sensor applications," *Thin Solid Films*, vol. 255, pp. 310–312, 1995.

[58] T. Taliercio, M. Dilhan, E. Massone, A. Foucaran, A. Gué, T. Bretagnon, B. Fraisse, and L. Montès, "Porous silicon membranes for gas-sensor applications," *Sensors Actuators A Phys.*, vol. 46, pp. 43–46, 1995.

[59] I. Schechter, M. Ben-Chorin, and A. Kux, "Gas Sensing Properties of Porous Silicon," *Anal. Chem.*, vol. 67, pp. 3727–3732, 1995.

[60] A. Motohashi, M. Kawakami, H. Aoyagi, A. Kinoshita, and A. Satou, "Gas Identification by a Single Gas Sensor using Porous Silicon as the Sensitive Material," *Jpn. J. Appl. Phys.*, vol. 34, pp. 5840–5843, 1995.

[61] V. S. Y. Lin, K. Motesharei, K. P. S. Dancil, M. J. Sailor, and M. R. Ghadiri, "A Porous Silicon-Based Optical Interferometric Biosensor," *Science (80-.).*, vol. 278, pp. 840–843, 1997.

[62] J. M. Buriak and M. J. Allen, "Lewis acid mediated functionalization of porous silicon with substituted alkenes and alkynes," *J. Am. Chem. Soc.*, vol. 120, pp. 1339–1340, 1998.

[63] R. Boukherroub, S. Morin, F. Bensebaa, and D. D. M. Wayner, "New synthetic routes to alkyl monolayers on the Si(111) surface," *Langmuir*, vol. 15, pp. 3831–3835, 1999.

[64] M. P. Stewart and J. M. Buriak, "Chemical and biological applications of porous silicon technology," *Adv. Mater.*, vol. 12, pp. 859–869, 2000.

[65] A. Jane, R. Dronov, A. Hodges, and N. H. Voelcker, "Porous silicon biosensors on the advance," *Trends Biotechnol.*, vol. 27, pp. 230–239, 2009.

[66] C. Chiappini, E. Tasciotti, J. R. Fakhoury, D. Fine, L. Pullan, Y.-C. Wang, L. Fu, X. Liu, and M. Ferrari, "Tailored porous silicon microparticles: fabrication and properties.," *Chemphyschem*, vol. 11, pp. 1029–1035, 2010.

[67] L. Osminkina, A. Nikolaev, A. Sviridov, N. Andronova, K. Tamarov, M. Gongalsky, A. Kudryavtsev, H. Treshalina, and V. Timoshenko, "Porous silicon nanoparticles as efficient sensitizers for sonodynamic therapy of cancer," *Microporous Mesoporous Mater.*, vol. 210, pp. 169–175, 2015.

[68] M. J. J. Theunissen, J. A. Appels, and W. H. C. G. Verkuylen, "Application of Preferential Electrochemical Etching of Silicon to Semiconductor Device Technology," *J. Electrochem. Soc.*, vol. 117, pp. 959–965, 1970.

[69] M. J. J. Theunissen, "Etch Channel Formation during Anodic Dissolution of N-Type Silicon in Aqueous Hydrofluoric Acid," *J. Electrochem. Soc.*, vol. 119, pp. 351–360, 1972.

[70] E. Hourdakis and A. G. Nassiopoulou, "A thermoelectric generator using porous Si thermal isolation.," *Sensors*, vol. 13, pp. 13596–13608, 2013.

[71] L. T. Canham, "Nanoscale semiconducting silicon as a nutritional food additive," *Nanotechnology*, vol. 18, p. 185704, 2007.

[72] J. P. Proot, C. Delerue, and G. Allan, "Electronic structure and optical properties of silicon crystallites: Application to porous silicon," *Appl. Phys. Lett.*, vol. 61, pp. 1948–1950, 1992.

[73] L. T. Canham, T. I. Cox, A. Loni, and A. J. Simons, "Progress towards silicon optoelectronics using porous silicon technology," *Appl. Surf. Sci.*, vol. 102, pp. 436–441, 1996.

[74] K. D. Hirschman, L. Tsybeskov, S. P. Duttagupta, and P. M. Fauchet, "Silicon-based visible light-emitting devices integrated into microelectronic circuits," *Nature*, vol. 384, pp. 338–341, 1996.

[75] D. A. B. Miller, "Silicon integrated circuits shine," *Nature*, vol. 384, pp. 307–308, 1996.

[76] A. Loni, L. Canham, M. Berger, R. Arens-Fischer, H. Munder, H. Luth, H. Arrand, and T. Benson, "Porous silicon multilayer optical waveguides," *Thin Solid Films*, vol. 276, pp. 143–146, 1996.

[77] R. T. Collins, P. M. Fauchet, and M. A. Tischler, "Porous silicon: From luminescence to LEDs," *Phys. Today*, vol. 50, pp. 24–31, 1997.

[78] V. Parkhutik, "Porous silicon - mechanisms of growth and applications," *Solid. State. Electron.*, vol. 43, pp. 1121–1141, 1999.

[79] C. H. Chen and Y. F. Chen, "Strong and stable visible luminescence from Au-passivated porous silicon," *Appl. Phys. Lett.*, vol. 75, pp. 2560–2562, 1999.

[80] L. Montès and R. Hérino, "Luminescence and structural properties of porous silicon with ZnSe intimate contact," *Mater. Sci. Eng. B*, vol. 69-70, pp. 136–141, 2000.

[81] R. Boukherroub, D. D. M. Wayner, D. J. Lockwood, and L. T. Canham, "Passivated luminescent porous silicon," *J. Electrochem. Soc.*, vol. 148, pp. H91—-H97, 2001.

[82] R. Boukherroub, S. Morin, D. D. M. Wayner, F. Bensebaa, G. I. Sproule, J. M. Baribeau, and D. J. Lockwood, "Ideal passivation of luminescent porous silicon by thermal, noncatalytic reaction with alkenes and aldehydes," *Chem. Mater.*, vol. 13, pp. 2002–2011, 2001.

[83] M. P. Stewart and J. M. Buriak, "Exciton-Mediated Hydrosilylation on Photoluminescent Nanocrystalline Silicon," *J. Am. Chem. Soc.*, vol. 123, pp. 7821–7830, 2001.

[84] N. Taghavinia, G. Lerondel, H. Makino, A. Parisini, A. Yamamoto, T. Yao, Y. Kawazoe, and T. Goto, "Activation of porous silicon layers using Zn2SiO4:Mn2+ phosphor particles," *J. Lumin.*, vol. 96, pp. 171–175, 2002.

[85] A. M. Morales and C. M. Lieber, "A Laser Ablation Method for the Synthesis of Crystalline Semiconductor Nanowires," *Science (80-.).*, vol. 279, pp. 208–211, 1998.

[86] J. Fan, X. Wu, and P. K. Chu, "Low-dimensional SiC nanostructures: Fabrication, luminescence, and electrical properties," *Prog. Mater. Sci.*, vol. 51, pp. 983–1031, 2006.

[87] L. T. Canham, "Luminescent Bands and Their Proposed Origins In Highly Porous Silicon," *Phys. Status Solidi B-basic Res.*, vol. 190, pp. 9–14, 1995.

[88] P. Li, C. Ohtsuki, T. Kokubo, K. Nakanishi, N. Soga, T. Nakamura, and T. Yamamuro, "Apatite Formation Induced by Silica Gel in a Simulated Body Fluid," *J. Am. Ceram. Soc.*, vol. 75, pp. 2094–2097, 1992.

[89] L. T. Canham, A. Loni, P. D. J. Calcott, A. J. Simons, C. Reeves, M. R. Houlton, J. P. Newey, K. J. Nash, and T. I. Cox, "On the origin of blue luminescence arising from atmospheric impregnation of oxidized porous silicon," *Thin Solid Films*, vol. 276, pp. 112–115, 1996.

[90] L. T. Canham, C. L. Reeves, A. Loni, M. R. Houlton, J. P. Newey, A. J. Simons, and T. I. Cox, "Calcium phosphate nucleation on porous silicon: Factors influencing kinetics in acellular simulated body fluids," *Thin Solid Films*, vol. 297, pp. 304–307, 1997.

[91] S. Bayliss, L. Buckberry, P. Harris, and C. Rousseau, "Nanostructured semiconductors: compatibility with biomaterials," *Thin Solid Films*, vol. 297, pp. 308–310, 1997.

[92] X. Li, J. L. Coffer, Y. D. Chen, R. F. Pinizzotto, J. Newey, and L. T. Canham, "Transition metal complex-doped hydroxyapatite layers on porous silicon," *J. Am. Chem. Soc.*, vol. 120, pp. 11706–11709, 1998.

[93] S. Bayliss, L. Buckberry, I. Fletcher, and M. Tobin, "The culture of neurons on silicon," *Sensors Actuators A Phys.*, vol. 74, pp. 139–142, 1999.

[94] L. T. Canham, C. L. Reeves, J. P. Newey, M. R. Houlton, T. I. Cox, J. M. Buriak, and M. P. Stewart, "Derivatized Mesoporous Silicon with

Dramatically Improved Stability in Simulated Human Blood Plasma," *Adv. Mater.*, vol. 11, pp. 1505–1507, 1999.

[95] L. Canham, "Gaining light from silicon," *Nature*, vol. 408, pp. 411–412, 2000.

[96] A. Rosengren, L. Wallman, M. Bengtsson, T. Laurell, N. Danielsen, and L. Bjursten, "Tissue Reactions to Porous Silicon: A Comparative Biomaterial Study," *Phys. status solidi*, vol. 182, pp. 527–531, 2000.

[97] S. H. C. Anderson, H. Elliott, D. J. Wallis, L. T. Canham, and J. J. Powell, "Dissolution of different forms of partially porous silicon wafers under simulated physiological conditions," *Phys. Status Solidi A-applied Res.*, vol. 197, pp. 331–335, 2003.

[98] J. L. Coffer, J.-L. Montchamp, J. B. Aimone, and R. P. Weis, "Routes to calcified porous silicon: implications for drug delivery and biosensing," *Phys. status solidi*, vol. 197, pp. 336–339, 2003.

[99] J.-H. Park, L. Gu, G. von Maltzahn, E. Ruoslahti, S. N. Bhatia, and M. J. Sailor, "Biodegradable luminescent porous silicon nanoparticles for in vivo applications," *Nat. Mater.*, vol. 8, pp. 331–336, 2009.

[100] S. P. Low, N. H. Voelcker, L. T. Canham, and K. A. Williams, "The biocompatibility of porous silicon in tissues of the eye," *Biomaterials*, vol. 30, pp. 2873–2880, 2009.

[101] M.-A. Shahbazi, M. Hamidi, E. M. Mäkilä, H. Zhang, P. V. Almeida, M. Kaasalainen, J. J. Salonen, J. T. Hirvonen, and H. A. Santos, "The mechanisms of surface chemistry effects of mesoporous silicon nanoparticles on immunotoxicity and biocompatibility," *Biomaterials*, vol. 34, pp. 7776–7789, 2013.

[102] M. A. Tölli, M. P. A. Ferreira, S. M. Kinnunen, J. Rysä, E. M. Mäkilä, Z. Szabó, R. E. Serpi, P. J. Ohukainen, M. J. Välimäki, A. M. R. Correia, J. J. Salonen, J. T. Hirvonen, H. J. Ruskoaho, and H. A. Santos, "In vivo biocompatibility of porous silicon biomaterials for drug delivery to the heart.," *Biomaterials*, vol. 35, pp. 8394–405, 2014.

[103] M.-A. Shahbazi, T. D. Fernández, E. M. Mäkilä, X. Le Guével, C. Mayorga, M. H. Kaasalainen, J. J. Salonen, J. T. Hirvonen, and H. A.

Santos, "Surface chemistry dependent immunostimulative potential of porous silicon nanoplatforms," *Biomaterials*, vol. 35, pp. 9224–9235, 2014.

[104] L. Pramatarova, E. Pecheva, D. Dimova-Malinovska, R. Pramatarova, U. Bismayer, T. Petrov, and N. Minkovski, "Porous silicon as a substrate for hydroxyapatite growth," *Vacuum*, vol. 76, pp. 135–138, 2004.

[105] J. L. Coffer, M. A. Whitehead, D. K. Nagesha, P. Mukherjee, G. Akkaraju, M. Totolici, R. S. Saffie, and L. T. Canham, "Porous silicon-based scaffolds for tissue engineering and other biomedical applications," *Phys. Status Solidi A-applications Mater. Sci.*, vol. 202, pp. 1451–1455, 2005.

[106] M. A. Whitehead, D. Fan, P. Mukherjee, G. R. Akkaraju, L. T. Canham, and J. L. Coffer, "High-porosity poly(epsilon-caprolactone)/mesoporous silicon scaffolds: Calcium phosphate deposition and biological response to bone precursor cells," *Tissue Eng. Part A*, vol. 14, pp. 195–206, 2008.

[107] K. Bodišová, M. Kašiarová, M. Domanická, M. Hnatko, Z. Lenčéš, Z. V. Nováková, J. Vojtaššák, S. Gromošová, and P. Šajgalík, "Porous silicon nitride ceramics designed for bone substitute applications," *Ceram. Int.*, vol. 39, pp. 8355–8362, 2013.

[108] M. López-Álvarez, C. Rodríguez-Valencia, J. Serra, and P. González, "Bio-inspired Ceramics: Promising Scaffolds for Bone Tissue Engineering," *Procedia Eng.*, vol. 59, pp. 51–58, 2013.

[109] J. Hernandez-Montelongo, D. Gallach, N. Naveas, V. Torres-Costa, A. Climent-Font, J. P. García-Ruiz, and M. Manso-Silvan, "Calcium phosphate/porous silicon biocomposites prepared by cyclic deposition methods: spin coating vs electrochemical activation.," *Mater. Sci. Eng. C. Mater. Biol. Appl.*, vol. 34, pp. 245–51, 2014.

[110] F. Caruso, "Nanoengineering of Particle Surfaces," *Adv. Mater.*, vol. 13, pp. 11–22, 2001.

[111] M. Vallet-Regi, A. Rámila, R. P. del Real, and J. Pérez-Pariente, "A New Property of MCM-41: Drug Delivery System," *Chem. Mater.*, vol. 13, pp. 308–311, 2001.

[112] S. Zangooie, R. Bjorklund, and H. Arwin, "Protein adsorption in thermally oxidized porous silicon layers," *Thin Solid Films*, vol. 313-314, pp. 825–830, 1998.

[113] A. B. Foraker, R. J. Walczak, M. H. Cohen, T. A. Boiarski, C. F. Grove, and P. W. Swaan, "Microfabricated Porous Silicon Particles Enhance Paracellular Delivery of Insulin across Intestinal Caco-2 Cell Monolayers," *Pharm. Res.*, vol. 20, pp. 110–116, 2003.

[114] X. Li, J. St. John, J. L. Coffer, Y. Chen, R. F. Pinizzotto, J. Newey, C. Reeves, and L. T. Canham, "Porosified Silicon Wafer Structures Impregnated With Platinum Anti-Tumor Compounds: Fabrication, Characterization, and Diffusion Studies," *Biomed. Microdevices*, vol. 2, pp. 265–272, 2000.

[115] R. R. P. Weis, J. J. L. Montchamp, J. J. L. Coffer, D. G. D. Attiah, and T. T. A. Desai, "Calcified nanostructured silicon wafer surfaces for biosensing: Effects of surface modification on bioactivity," *Dis. Markers*, vol. 18, pp. 159–165, 2002.

[116] J. Salonen, L. Laitinen, A. Kaukonen, J. Tuura, M. Björkqvist, T. Heikkilä, K. Vähä-Heikkilä, J. Hirvonen, and V.-P. Lehto, "Mesoporous silicon microparticles for oral drug delivery: Loading and release of five model drugs," *J. Control. Release*, vol. 108, pp. 362–374, 2005.

[117] E. J. Anglin, L. Y. Cheng, W. R. Freeman, and M. J. Sailor, "Porous silicon in drug delivery devices and materials," *Adv. Drug Deliv. Rev.*, vol. 60, pp. 1266–1277, 2008.

[118] E. C. Wu, J. H. Park, J. Park, E. Segal, F. Cunin, and M. J. Sailor, "Oxidation-Triggered Release of Fluorescent Molecules or Drugs from Mesoporous Si Microplarticles," *ACS Nano*, vol. 2, pp. 2401–2409, 2008.

[119] A. M. Kaukonen, L. Laitinen, J. Salonen, J. Tuura, T. Heikkilä, T. Limnell, J. Hirvonen, and V.-P. Lehto, "Enhanced in vitro permeation of furosemide loaded into thermally carbonized mesoporous silicon (TCPSi) microparticles," *Eur. J. Pharm. Biopharm.*, vol. 66, pp. 348–356, 2007.

[120] M. Kilpeläinen, J. Mönkäre, M. A. Vlasova, J. Riikonen, V.-P. Lehto, J. Salonen, K. Järvinen, and K.-H. Herzig, "Nanostructured porous silicon microparticles enable sustained peptide (Melanotan II) delivery," *Eur. J. Pharm. Biopharm.*, vol. 77, pp. 20–25, 2011.

[121] C.-F. Wang, E. M. Mäkilä, M. H. Kaasalainen, M. V. Hagström, J. J. Salonen, J. T. Hirvonen, and H. A. Santos, "Dual-drug delivery by porous silicon nanoparticles for improved cellular uptake, sustained release, and combination therapy," *Acta Biomater.*, vol. 16, pp. 206–214, 2015.

[122] L. Gu, J.-H. Park, K. H. Duong, E. Ruoslahti, and M. J. Sailor, "Magnetic Luminescent Porous Silicon Microparticles for Localized Delivery of Molecular Drug Payloads," *Small*, vol. 6, pp. 2546–2552, 2010.

[123] L. M. Bimbo, E. Mäkilä, J. Raula, T. Laaksonen, P. Laaksonen, K. Strommer, E. I. Kauppinen, J. Salonen, M. B. Linder, J. Hirvonen, and H. A. Santos, "Functional hydrophobin-coating of thermally hydrocarbonized porous silicon microparticles," *Biomaterials*, vol. 32, pp. 9089–9099, 2011.

[124] M. Kaasalainen, E. Mäkilä, J. Riikonen, M. Kovalainen, K. Järvinen, K.-H. Herzig, V.-P. Lehto, and J. Salonen, "Effect of isotonic solutions and peptide adsorption on zeta potential of porous silicon nanoparticle drug delivery formulations.," *Int. J. Pharm.*, vol. 431, pp. 230–236, 2012.

[125] J. Roine, M. Murtomaa, M. Myllys, and J. Salonen, "Dual-capillary electroencapsulation of mesoporous silicon drug carrier particles for controlled oral drug delivery," *J. Electrostat.*, vol. 70, pp. 428–437, 2012.

[126] P. J. Kinnari, M. L. Hyvönen, E. M. Mäkilä, M. H. Kaasalainen, A. Rivinoja, J. J. Salonen, J. T. Hirvonen, P. M. Laakkonen, and H. A. Santos, "Tumour homing peptide-functionalized porous silicon nanovectors for cancer therapy," *Biomaterials*, vol. 34, pp. 9134–9141, 2013.

[127] N. Shrestha, M.-A. Shahbazi, F. Araújo, H. Zhang, E. M. Mäkilä, J. Kauppila, B. Sarmento, J. J. Salonen, J. T. Hirvonen, and H. A. Santos, "Chitosan-modified porous silicon microparticles for enhanced

permeability of insulin across intestinal cell monolayers.," *Biomaterials*, vol. 35, pp. 7172–9, 2014.

[128] M. Kovalainen, J. Monkare, J. Riikonen, U. Pesonen, M. Vlasova, J. Salonen, V.-P. Lehto, K. Jarvinen, and K.-H. Herzig, "Novel Delivery Systems for Improving the Clinical Use of Peptides," *Pharmacol. Rev.*, vol. 67, pp. 541–561, 2015.

[129] J. W. Mares, J. S. Fain, K. R. Beavers, C. L. Duvall, and S. M. Weiss, "Shape-Engineered multifunctional porous silicon nanoparticles by direct imprinting," *Nanotechnology*, vol. 26, pp. 71001–71001, 2015.

[130] M. Baranowska, A. J. Slota, P. J. Eravuchira, M. Alba, P. Formentin, J. Pallarès, J. Ferré-Borrull, and L. F. Marsal, "Protein attachment to silane-functionalized porous silicon: A comparison of electrostatic and covalent attachment," *J. Colloid Interface Sci.*, vol. 452, pp. 180–189, 2015.

[131] J. Riikonen, A. Correia, M. Kovalainen, S. Näkki, M. Lehtonen, J. Leppänen, J. Rantanen, W. Xu, F. Araújo, J. Hirvonen, K. Järvinen, H. A. Santos, and V.-P. Lehto, "Systematic in vitro and in vivo study on porous silicon to improve the oral bioavailability of celecoxib.," *Biomaterials*, vol. 52, pp. 44–55, 2015.

[132] C.-F. Wang, M. P. Sarparanta, E. M. Mäkilä, M. L. Hyvönen, P. M. Laakkonen, J. J. Salonen, J. T. Hirvonen, A. J. Airaksinen, and H. A. Santos, "Multifunctional porous silicon nanoparticles for cancer theranostics," *Biomaterials*, vol. 48, pp. 108–118, 2015.

[133] Z. Y. Xu, M. Gal, and M. Gross, "Photoluminescence studies on porous silicon," *Appl. Phys. Lett.*, vol. 60, pp. 1375–1377, mar 1992.

[134] J. M. Lauerhaas and M. J. Sailor, "Chemical Modification of the Photoluminescence Quenching of Porous Silicon," *Science (80-.).*, vol. 261, pp. 1567–1568, 1993.

[135] J. L. Coffer, S. C. Lilley, R. A. Martin, and L. A. FilesSesler, "Surface reactivity of luminescent porous silicon," *J. Appl. Phys.*, vol. 74, pp. 2094–2096, 1993.

[136] M. Ben-Chorin, A. Kux, and I. Schechter, "Adsorbate effects on photoluminescence and electrical conductivity of porous silicon," *Appl. Phys. Lett.*, vol. 64, pp. 481–483, 1994.

[137] M. T. Kelly and A. B. Bocarsly, "Mechanisms of photoluminescent quenching of oxidized porous silicon - Applications to chemical sensing," *Coord. Chem. Rev.*, vol. 171, pp. 251–259, 1998.

[138] S. Content, W. W. C. Trogler, and M. M. J. Sailor, "Detection of nitrobenzene, DNT, and TNT vapors by quenching of porous silicon photoluminescence," *Chem. - A Eur. J.*, vol. 6, pp. 2205–2213, 2000.

[139] S. Chan and P. M. Fauchet, "Silicon microcavity light emitting devices," *Opt. Mater. (Amst).*, vol. 17, pp. 31–34, 2001.

[140] M. Björkqvist, J. Salonen, E. Laine, and L. Niinistö, "Comparison of stabilizing treatments on porous silicon for sensor applications," *Phys. status solidi*, vol. 197, pp. 374–377, 2003.

[141] M. Björkqvist, J. Salonen, J. Paski, and E. Laine, "Characterization of thermally carbonized porous silicon humidity sensor," *Sensors Actuators A Phys.*, vol. 112, pp. 244–247, 2004.

[142] S. E. Lewis, J. R. DeBoer, J. L. Gole, and P. J. Hesketh, "Sensitive, selective, and analytical improvements to a porous silicon gas sensor," *Sensors Actuators B Chem.*, vol. 110, pp. 54–65, 2005.

[143] T. Jalkanen, J. Tuura, E. Mäkilä, and J. Salonen, "Electro-optical porous silicon gas sensor with enhanced selectivity," *Sensors Actuators B Chem.*, vol. 147, pp. 100–104, may 2010.

[144] S. Hilbrich, R. Arens-Fischer, L. Küpper, W. Theiß, M. G. Berger, M. Krüger, M. Thönissen, R. ArensFischer, L. Kupper, W. Theiss, M. G. Berger, M. Kruger, and M. Thonissen, "The application of porous silicon interference filters in optical sensors," *Thin Solid Films*, vol. 297, pp. 250–253, 1997.

[145] A. Janshoff, K.-P. S. P. S. Dancil, C. Steinem, D. P. Greiner, V. S.-Y. Y. Lin, C. Gurtner, K. Motesharei, M. J. Sailor, and M. R. Ghadiri,

"Macroporous p-Type Silicon FabryPerot Layers. Fabrication, Characterization, and Applications in Biosensing," *J. Am. Chem. Soc.*, vol. 120, pp. 12108–12116, 1998.

[146] P. Allcock and P. A. Snow, "Time-resolved sensing of organic vapors in low modulating porous silicon dielectric mirrors," *J. Appl. Phys.*, vol. 90, pp. 5052–5057, 2001.

[147] P. A. Snow, E. K. Squire, P. S. J. Russell, and L. T. Canham, "Vapor sensing using the optical properties of porous silicon Bragg mirrors," *J. Appl. Phys.*, vol. 86, p. 1781, 1999.

[148] V. Mulloni, Z. Gaburro, and L. Pavesi, "Porous silicon microcavities as optical and electrical chemical sensors," *Phys. Status Solidi A-applied Res.*, vol. 182, pp. 479–484, 2000.

[149] X. Li, Y. He, S. S. Talukdar, and M. T. Swihart, "Process for Preparing Macroscopic Quantities of Brightly Photoluminescent Silicon Nanoparticles with Emission Spanning the Visible Spectrum," *Langmuir*, vol. 19, pp. 8490–8496, 2003.

[150] B. H. King, A. M. Ruminski, J. L. Snyder, and M. J. Sailor, "Optical-Fiber-Mounted Porous Silicon Photonic Crystals for Sensing Organic Vapor Breakthrough in Activated Carbon," *Adv. Mater.*, vol. 19, pp. 4530–4534, 2007.

[151] T. Jalkanen, E. Mäkilä, A. Määttänen, J. Tuura, M. Kaasalainen, V.-P. Lehto, P. Ihalainen, J. Peltonen, and J. Salonen, "Porous silicon micro- and nanoparticles for printed humidity sensors," *Appl. Phys. Lett.*, vol. 101, p. 263110, 2012.

[152] T. Jalkanen, A. Määttänen, E. Mäkilä, J. Tuura, M. Kaasalainen, V.-P. Lehto, P. Ihalainen, J. Peltonen, and J. Salonen, "Fabrication of Porous Silicon Based Humidity Sensing Elements on Paper," *J. Sensors*, vol. 2015, pp. 1–10, 2015.

[153] S. Ma, M. Hu, P. Zeng, M. Li, W. Yan, and Y. Qin, "Synthesis and low-temperature gas sensing properties of tungsten oxide nanowires/porous silicon composite," *Sensors Actuators B Chem.*, vol. 192, pp. 341–349, 2014.

[154] W. Wang, Y. Gao, Q. Tao, Y.-Z. Liu, J.-J. Zuo, X.-C. Ju, and J.-K. Zhang, "A Novel Porous Silicon Composite Sensor for Formaldehyde Detection," *Chinese J. Anal. Chem.*, vol. 43, pp. 849–855, 2015.

[155] H.-G. Kim and K.-W. Lee, "Electrostatic gas sensor with a porous silicon diaphragm," *Sensors Actuators B Chem.*, vol. 219, pp. 10–16, 2015.

[156] T. Blank, L. Eksperiandova, and K. Belikov, "Recent trends of ceramic humidity sensors development: A review," *Sensors Actuators B Chem.*, vol. 228, pp. 416–442, 2016.

[157] H. Kim, B. Han, J. Choo, and J. Cho, "Three-Dimensional Porous Silicon Particles for Use in High-Performance Lithium Secondary Batteries," *Angew. Chemie Int. Ed.*, vol. 47, pp. 10151–10154, 2008.

[158] Y. Yu, L. Gu, C. Zhu, S. Tsukimoto, P. A. van Aken, and J. Maier, "Reversible Storage of Lithium in Silver-Coated Three-Dimensional Macroporous Silicon," *Adv. Mater.*, vol. 22, pp. 2247–2250, 2010.

[159] X. Li, P. Meduri, X. Chen, W. Qi, M. H. Engelhard, W. Xu, F. Ding, J. Xiao, W. Wang, C. Wang, J.-G. Zhang, and J. Liu, "Hollow coreshell structured porous SiC nanocomposites for Li-ion battery anodes," *J. Mater. Chem.*, vol. 22, pp. 11014–11017, 2012.

[160] A. S. Aricò, P. Bruce, B. Scrosati, J.-M. Tarascon, and W. van Schalkwijk, "Nanostructured materials for advanced energy conversion and storage devices," *Nat. Mater.*, vol. 4, pp. 366–377, 2005.

[161] N.-L. Wu, "Porous Silicon and Li-Ion Batteries," in *Handb. Porous Silicon* (L. Canham, ed.), pp. 965–973, Zug: Springer International Publishing, 2014.

[162] B. Hertzberg, A. Alexeev, and G. Yushin, "Deformations in SiLi Anodes Upon Electrochemical Alloying in Nano-Confined Space," *J. Am. Chem. Soc.*, vol. 132, pp. 8548–8549, 2010.

[163] L. Canham, "Porous Silicon Formation by Porous Silica Reduction," in *Handb. Porous Silicon* (L. Canham, ed.), pp. 85–92, Zug: Springer International Publishing, 2014.

[164] G. Gautier, "Porous Silicon and Micro-Fuel Cells," in *Handb. Porous Silicon* (L. Canham, ed.), pp. 957–964, Zug: Springer International Publishing, 2014.

[165] T. Dzhafarov, "Porous Silicon and Solar Cells," in *Handb. Porous Silicon* (L. Canham, ed.), pp. 945–955, Zug: Springer International Publishing, 2014.

[166] K. Sakaguchii, "Current progress in epitaxial layer transfer eltran," *IEICE Trans. Electron.*, vol. E80-C, pp. 378–386, 1997.

[167] F. Hedrich, S. Billat, and W. Lang, "Structuring of membrane sensors using sacrificial porous silicon," *Sensors and Actuators A-physical*, vol. 84, pp. 315–323, 2000.

[168] Y. Y. Li, "Polymer Replicas of Photonic Porous Silicon for Sensing and Drug Delivery Applications," *Science (80-.).*, vol. 299, pp. 2045–2047, 2003.

[169] L. F. Marsal, P. Formentín, R. Palacios, T. Trifonov, J. Ferré-Borrull, A. Rodriguez, J. Pallarés, and R. Alcubilla, "Polymer microfibers obtained using porous silicon templates," *Phys. status solidi*, vol. 205, pp. 2437–2440, 2008.

[170] M. J. Sailor, *Porous Silicon in Practice*. Weinheim, Germany: Wiley-VCH Verlag GmbH & Co. KGaA, 2012.

[171] A. Loni, "Porous Silicon Formation by Anodization," in *Handb. Porous Silicon* (L. Canham, ed.), pp. 11–22, Zug: Springer International Publishing, 2014.

[172] G. Korotcenkov and B. K. Cho, "Silicon Porosification: State of the Art," *Crit. Rev. SOLID STATE Mater. Sci.*, vol. 35, pp. 153–260, 2010.

[173] K. W. Kolasinski, "Porous Silicon Formation by Galvanic Etching," in *Handb. Porous Silicon* (L. Canham, ed.), pp. 23–33, Zug: Springer International Publishing, 2014.

[174] K. W. Kolasinski, "Porous Silicon Formation by Stain Etching," in *Handb. Porous Silicon* (L. Canham, ed.), pp. 35–48, Zug: Springer International Publishing, 2014.

[175] C. Lévy-Clément, "Porous Silicon Formation by Metal Nanoparticle-Assisted Etching," in *Handb. Porous Silicon* (L. Canham, ed.), pp. 49–66, Zug: Springer International Publishing, 2014.

[176] B. Bessaïs, "Porous Silicon Formation by HNO3/HF Vapor Etching," in *Handb. Porous Silicon* (L. Canham, ed.), pp. 75–83, Zug: Springer International Publishing, 2014.

[177] V. Lehmann, *Electrochemistry of Silicon*. Weinheim, Germany: Wiley-VCH Verlag GmbH, 2002.

[178] C. Tsai, K. Li, D. S. Kinosky, R. Qian, T. Hsu, J. T. Irby, S. K. Banerjee, A. F. Tasch, J. C. Campbell, B. K. Hance, and J. M. White, "Correlation between silicon hydride species and the photoluminescence intensity of porous silicon," *Appl. Phys. Lett.*, vol. 60, pp. 1700–1702, 1992.

[179] J. Salonen, V.-P. Lehto, M. Björkqvist, and E. Laine, "A role of illumination during etching to porous silicon oxidation," *Appl. Phys. Lett.*, vol. 75, pp. 826–828, 1999.

[180] R. Mlcak, H. Tuller, P. Greiff, J. Sohn, and L. Niles, "Photoassisted electrochemical micromachining of silicon in HF electrolytes," *Sensors Actuators A Phys.*, vol. 40, pp. 49–55, 1994.

[181] X. G. Zhang, "Modern Aspects of Electrochemistry," in *Mod. Asp. Electrochem.* (C. G. Vayenas, R. E. White, and M. E. Gamboa-Adelco, eds.), vol. 39 of *Modern Aspects of Electrochemistry*, pp. 65–133, Boston, MA: Springer US, 2006.

[182] K. Kordás, J. Remes, S. Beke, T. Hu, and S. Leppävuori, "Manufacturing of porous silicon; porosity and thickness dependence on electrolyte composition," *Appl. Surf. Sci.*, vol. 178, pp. 190–193, 2001.

[183] M. Christophersen, J. Carstensen, A. Feuerhake, and H. Föll, "Crystal orientation and electrolyte dependence for macropore nucleation and stable growth on p-type Si," *Mater. Sci. Eng. B*, vol. 69-70, pp. 194–198, 2000.

[184] M. Christophersen, J. Carstensen, S. Rönnebeck, C. Jäger, W. Jäger, and H. Föll, "Crystal Orientation Dependence and Anisotropic Properties of Macropore Formation of p- and n-Type Silicon," *J. Electrochem. Soc.*, vol. 148, pp. E267–E275, 2001.

[185] C. Mazzoleni and L. Pavesi, "Application to optical components of dielectric porous silicon multilayers," *Appl. Phys. Lett.*, vol. 67, pp. 2983–2985, 1995.

[186] M. Berger, R. Arens-Fischer, M. Thönissen, M. Krüger, S. Billat, H. Lüth, S. Hilbrich, W. Theiß, and P. Grosse, "Dielectric filters made of PS: advanced performance by oxidation and new layer structures," *Thin Solid Films*, vol. 297, pp. 237–240, 1997.

[187] E. Lorenzo, C. J. Oton, N. E. Capuj, M. Ghulinyan, D. Navarro-Urrios, Z. Gaburro, and L. Pavesi, "Porous silicon-based rugate filters," *Appl. Opt.*, vol. 44, pp. 5415–5421, 2005.

[188] S. Ilyas, T. Böcking, K. Kilian, P. Reece, J. Gooding, K. Gaus, and M. Gal, "Porous silicon based narrow line-width rugate filters," *Opt. Mater. (Amst).*, vol. 29, pp. 619–622, 2007.

[189] A. M. Ruminski, B. H. King, J. Salonen, J. L. Snyder, and M. J. Sailor, "Porous Silicon-Based Optical Microsensors for Volatile Organic Analytes: Effect of Surface Chemistry on Stability and Specificity," *Adv. Funct. Mater.*, vol. 20, pp. 2874–2883, 2010.

[190] E. C. Wu, J. S. Andrew, L. Cheng, W. R. Freeman, L. Pearson, and M. J. Sailor, "Real-time monitoring of sustained drug release using the optical properties of porous silicon photonic crystal particles," *Biomaterials*, vol. 32, pp. 1957–1966, 2011.

[191] T. Jalkanen, V. Torres-Costa, E. Mäkilä, M. Kaasalainen, R. Koda, T. Sakka, Y. H. Ogata, and J. Salonen, "Selective Optical Response of Hydrolytically Stable Stratified Si Rugate Mirrors to Liquid Infiltration," *ACS Appl. Mater. Interfaces*, vol. 6, pp. 2884–2892, 2014.

[192] R. L. Smith, S. F. Chuang, and S. D. Collins, "A Theoretical-model of the Formation Morphologies of Porous Silicon," *J. Electron. Mater.*, vol. 17, pp. 533–541, 1988.

[193] V. Lehmann, "Formation Mechanism and Properties of Electrochemically Etched Trenches in n-Type Silicon," *J. Electrochem. Soc.*, vol. 137, pp. 653–659, 1990.

[194] P. Allongue, V. Kieling, and H. Gerischer, "Etching mechanism and atomic structure of HSi(111) surfaces prepared in NH4F," *Electrochim. Acta*, vol. 40, pp. 1353–1360, 1995.

[195] A. Valance, "Porous silicon formation: Stability analysis of the silicon-electrolyte interface," *Phys. Rev. B*, vol. 52, pp. 8323–8336, 1995.

[196] J. Carstensen, M. Christophersen, and H. Föll, "Pore formation mechanisms for the Si-HF system," *Mater. Sci. Eng. B*, vol. 69-70, pp. 23–28, 2000.

[197] J. N. Chazalviel and F. Ozanam, "Theory for the resonant response of an electrochemical system: self-oscillating domains, hidden oscillation, and synchronization impedance," *J. Electrochem. Soc.*, vol. 139, pp. 2501–2508, 1992.

[198] T. Unagami, "Oxidation of Porous Silicon and Properties of Its Oxide Film," *Jpn. J. Appl. Phys.*, vol. 19, pp. 231–241, 1980.

[199] Y. Kato, T. Ito, and A. Hiraki, "Low temperature oxidation of crystalline porous silicon," *Appl. Surf. Sci.*, vol. 41-42, pp. 614–618, 1990.

[200] N. Zoubir, M. Vergnat, T. Delatour, A. Burneau, P. De Donato, and O. Barrès, "Natural oxidation of annealed chemically etched porous silicon," *Thin Solid Films*, vol. 255, pp. 228–230, 1995.

[201] G. Mattei, E. V. Alieva, J. E. Petrov, and V. A. Yakovlev, "Quick oxidation of porous silicon in presence of pyridine vapor," *Phys. Status Solidi A-applied Res.*, vol. 182, pp. 139–143, 2000.

[202] E. V. Astrova, "Oxidation of Macroporous Silicon," in *Handb. Porous Silicon* (L. Canham, ed.), pp. 589–598, Zug: Springer International Publishing, 2014.

[203] K. Imai and H. Unno, "FIPOS (Full Isolation by Porous Oxidized Silicon) technology and its application to LSI's," *IEEE Trans. Electron Devices*, vol. 31, pp. 297–302, 1984.

[204] L. T. Canham, M. R. Houlton, W. Y. Lleong, C. Pickering, and J. M. Keen, "Atmospheric Impregnation of Porous Silicon At Room-temperature," *J. Appl. Phys.*, vol. 70, pp. 422–431, 1991.

[205] L. Tsybeskov, S. Duttagupta, and P. Fauchet, "Photoluminescence and electroluminescence in partially oxidized porous silicon," *Solid State Commun.*, vol. 95, pp. 429–433, 1995.

[206] J. Riikonen, M. Salomäki, J. van Wonderen, M. Kemell, W. Xu, O. Korhonen, M. Ritala, F. MacMillan, J. Salonen, and V.-P. Lehto, "Surface Chemistry, Reactivity, and Pore Structure of Porous Silicon Oxidized by Various Methods," *Langmuir*, vol. 28, pp. 10573–10583, 2012.

[207] A. Nakajima, T. Itakura, S. Watanabe, and N. Nakayama, "Photoluminescence of porous Si, oxidized then deoxidized chemically," *Appl. Phys. Lett.*, vol. 61, pp. 46–48, 1992.

[208] R. Vadjikar, B. Jain, P. Gupta, R. Nandedkar, D. Bhawalkar, M. Patni, R. Srinivasa, and A. Chandorkar, "Chemical treatment of photoluminescent porous silicon," *Mater. Sci. Eng. B*, vol. 23, pp. L13–L15, 1994.

[209] B. M. Rao, P. Basu, J. Biswas, S. Lahiri, S. Ghosh, and D. Bose, "Large enhancement of photoluminescence from porous silicon films by post-anodization treatment in boiling hydrogen peroxide," *Solid State Commun.*, vol. 97, pp. 417–418, 1996.

[210] G. Mattei, V. Valentini, and V. Yakovlev, "An FTIR study of porous silicon layers exposed to humid air with and without pyridine vapors at room temperature," *Surf. Sci.*, vol. 502-503, pp. 58–62, 2002.

[211] L. A. Osminkina, "Influence of Pyridine Molecule Adsorption on Concentrations of Free Carriers and Paramagnetic Centers in Porous Silicon Layers," *Semiconductors*, vol. 39, pp. 458–461, 2005.

[212] J. L. Cantin, M. Schoisswohl, A. Grosman, S. Lebib, C. Ortega, H. J. Von Bardeleben, É. Vázsonyi, G. Jalsovszky, and J. Erostyák, "Anodic oxidation of p- and p+-type porous silicon: Surface structural transformations and oxide formation," *Thin Solid Films*, vol. 276, pp. 76–79, 1996.

[213] K. Hamano, M. Sakamoto, and H. Yamanaka, "Oxidation Process of Porous Silicon," *Jpn. J. Appl. Phys.*, vol. 14, pp. 413–414, 1975.

[214] M. Hecini, A. Khelifa, B. Bouzid, N. Drouiche, S. Aoudj, and H. Hamitouche, "Study of formation, stabilization and properties of porous silicon and porous silica," *J. Phys. Chem. Solids*, vol. 74, pp. 1227–1234, 2013.

[215] Y. H. Ogata, "Characterization of Porous Silicon by Infrared Spectroscopy," in *Handb. Porous Silicon* (L. Canham, ed.), pp. 473–480, Zug: Springer International Publishing, 2014.

[216] D. B. Mawhinney, J. A. Glass, and J. T. Yates, "FTIR Study of the Oxidation of Porous Silicon," *J. Phys. Chem. B*, vol. 101, pp. 1202–1206, 1997.

[217] M. Fried, O. Polgár, T. Lohner, S. Strehlke, and C. Levy-Clement, "Comparative study of the oxidation of thin porous silicon layers studied by reflectometry, spectroscopic ellipsometry and secondary ion mass spectroscopy," *J. Lumin.*, vol. 80, pp. 147–152, 1998.

[218] J. J. Yon, K. Barla, R. Herino, and G. Bomchil, "The Kinetics and Mechanism of Oxide Layer Formation From Porous Silicon Formed On P-si Substrates," *J. Appl. Phys.*, vol. 62, pp. 1042–1048, 1987.

[219] P. Kan and T. Finstad, "Oxidation of macroporous silicon for thick thermal insulation," *Mater. Sci. Eng. B*, vol. 118, pp. 289–292, 2005.

[220] Y. Nakajima, A. Kojima, and N. Koshida, "Generation of ballistic electrons in nanocrystalline porous silicon layers and its application to a solid-state planar luminescent device," *Appl. Phys. Lett.*, vol. 81, pp. 2472–2474, 2002.

[221] U. Frotscher, U. Rossow, M. Ebert, C. Pietryga, W. Richter, M. G. Berger, R. Arens-Fischer, and H. Münder, "Investigation of different oxidation processes for porous silicon studied by spectroscopic ellipsometry," *Thin Solid Films*, vol. 276, pp. 36–39, 1996.

[222] V. Mulloni and L. Pavesi, "Electrochemically oxidised porous silicon microcavities," *Mater. Sci. Eng. B*, vol. 69-70, pp. 59–65, 2000.

[223] C. Lee, C. Yeh, and K. Hsu, "Formation of bottom oxides in porous silicon films by anodic oxidation," *Appl. Surf. Sci.*, vol. 92, pp. 621–625, 1996.

[224] M. Hory, R. Hérino, M. Ligeon, F. Muller, F. Gaspard, I. Mihalcescu, and J. Vial, "Fourier transform IR monitoring of porous silicon passivation during post-treatments such as anodic oxidation and contact with organic solvents," *Thin Solid Films*, vol. 255, pp. 200–203, 1995.

[225] V. Parkhutik, "Kinetics, composition and mechanism of anodic oxide growth on silicon in water-containing electrolytes," *Electrochim. Acta*, vol. 36, pp. 1611–1616, 1991.

[226] A. Bsiesy, F. Gaspard, R. Herino, M. Ligeon, F. Muller, and J. C. Oberlin, "Anodic oxidation of porous silicon layers formed on lightly p-doped substrates," *J. Electrochem. Soc.*, vol. 138, pp. 3450–3456, 1991.

[227] C. H. Lee, C. C. Yeh, H. L. Hwang, and K. Y. J. Hsu, "Characterization of porous silicon-on-insulator films prepared by anodic oxidation," *Thin Solid Films*, vol. 276, pp. 147–150, 1996.

[228] E. L. Pastor, J. A. Ayucar, J. Curiel-Esparza, E. S. Matveeva, J. Salonen, and V. P. Letho, "Electrochemical Oxidation of Mesoporous Silicon: Structural and Morphology Properties of the Obtained ox-porSi Material," *ECS Trans.*, vol. 6, pp. 23–34, 2007.

[229] Y. W. Chung, W. Siekhaus, and G. Somorjai, "Studies of acetylene and oxygen adsorption on silicon surfaces by low energy electron loss spectroscopy," *Surf. Sci.*, vol. 58, pp. 341–348, 1976.

[230] F. Smith and B. Meyerson, "Reactions of acetylene and ammonia with the Si(111) surface at high temperatures," *Thin Solid Films*, vol. 60, pp. 227–230, 1979.

[231] M. R. Linford and C. E. D. Chidsey, "Alkyl monolayers covalently bonded to silicon surfaces," *J. Am. Chem. Soc.*, vol. 115, pp. 12631–12632, 1993.

[232] T. Hatayama, Y. Tarui, T. Yoshinobu, T. Fuyuki, and H. Matsunami, "Controlled carbonization of Si(001) surface using hydrocarbon radicals in ultrahigh vacuum," *J. Cryst. Growth*, vol. 136, pp. 333–337, 1994.

[233] J. H. Song and M. J. Sailor, "Functionalization of Nanocrystalline Porous Silicon Surfaces with Aryllithium Reagents: Formation of SiliconCarbon Bonds by Cleavage of SiliconSilicon Bonds," *J. Am. Chem. Soc.*, vol. 120, pp. 2376–2381, 1998.

[234] J. M. Buriak and M. J. Allen, "Photoluminescence of porous silicon surfaces stabilized through Lewis acid mediated hydrosilylation," *J. Lumin.*, vol. 80, pp. 29–35, 1998.

[235] J. Salonen, E. Laine, and L. Niinisto, "Thermal carbonization of porous silicon surface by acetylene," *J. Appl. Phys.*, vol. 91, pp. 456–461, 2002.

[236] R. Boukherroub and D. D. M. Wayner, "Controlled functionalization and multistep chemical manipulation of covalently modified Si(111) surfaces," *J. Am. Chem. Soc.*, vol. 121, pp. 11513–11515, 1999.

[237] L. A. Huck and J. M. Buriak, "Silicon-Carbon Bond Formation on Porous Silicon," in *Handb. Porous Silicon* (L. Canham, ed.), pp. 683–693, Zug: Springer International Publishing, 2014.

[238] J. Salonen, V. P. Lehto, M. Björkqvist, E. Laine, and L. Niinisto, "Studies of thermally-carbonize porous silicon surfaces," *Phys. Status Solidi A-applied Res.*, vol. 182, pp. 123–126, 2000.

[239] J. Salonen, M. Björkqvist, E. Laine, and L. Niinistö, "Stabilization of porous silicon surface by thermal decomposition of acetylene," *Appl. Surf. Sci.*, vol. 225, pp. 389–394, 2004.

[240] J. Yoshinobu, H. Tsuda, M. Onchi, and M. Nishijima, "Rehybridization of acetylene on the Si(111) (7 7) surface - a vibrational study," *Chem. Phys. Lett.*, vol. 130, pp. 170–174, 1986.

[241] G. Dufour, F. Rochet, F. C. Stedile, C. Poncey, M. De Crescenzi, R. Gunnella, and M. Froment, "SiC formation by reaction of Si(001) with acetylene: Electronic structure and growth mode," *Phys. Rev. B - Condens. Matter Mater. Phys.*, vol. 56, pp. 4266–4282, 1997.

[242] F. Stedile, F. Rochet, C. Poncey, G. Dufour, R. Gunnella, M. De Crescenzi, and M. Froment, "First stages of low temperature and low pressure carbonization of Si (0 0 1) in acetylene," *Nucl. Instruments Methods Phys. Res. Sect. B Beam Interact. with Mater. Atoms*, vol. 136-138, pp. 301–307, 1998.

[243] C. K. Tsang, T. L. Kelly, M. J. Sailor, and Y. Y. Li, "Highly stable porous silicon-carbon composites as label-free optical biosensors.," *ACS Nano*, vol. 6, pp. 10546–54, 2012.

[244] J. Salonen, "Characterization of Porous Silicon by Calorimetry," in *Handb. Porous Silicon* (L. Canham, ed.), pp. 449–454, Zug: Springer International Publishing, 2014.

[245] M. J. Sailor, "Chemical Reactivity and Surface Chemistry of Porous Silicon," in *Handb. Porous Silicon* (L. Canham, ed.), pp. 355–380, Zug: Springer International Publishing, 2014.

[246] J. Salonen, M. Kaasalainen, O.-P. Rauhala, L. Lassila, M. Hakamies, T. Jalkanen, R. Hahn, P. Schmuki, and E. Makila, "(Invited) Thermal Carbonization of Porous Silicon: The Current Status and Recent Applications," *ECS Trans.*, vol. 69, pp. 167–176, 2015.

[247] L. Oakes, A. Westover, J. W. Mares, S. Chatterjee, W. R. Erwin, R. Bardhan, S. M. Weiss, and C. L. Pint, "Surface engineered porous silicon for stable, high performance electrochemical supercapacitors," *Sci. Rep.*, vol. 3, pp. 4863–4868, 2013.

[248] D. S. Gardner, C. W. Holzwarth, Y. Liu, S. B. Clendenning, W. Jin, B.-K. Moon, C. Pint, Z. Chen, E. C. Hannah, C. Chen, C. Wang, E. Mäkilä, R. Chen, T. Aldridge, and J. L. Gustafson, "Integrated on-chip energy storage using passivated nanoporous-silicon electrochemical capacitors," *Nano Energy*, vol. 25, pp. 68–79, 2016.

[249] R. Smith and S. Collins, "Thick films of silicon nitride," *Sensors Actuators A Phys.*, vol. 23, pp. 830–834, 1990.

[250] V. Morazzani, J. Cantin, C. Ortega, B. Pajot, R. Rahbi, M. Rosenbauer, H. von Bardeleben, and E. Vazsonyi, "Thermal nitridation of p-type porous silicon in ammonia," *Thin Solid Films*, vol. 276, pp. 32–35, 1996.

[251] M. Lai, G. Parish, Y. Liu, J. M. Dell, and A. J. Keating, "Development of an Alkaline-Compatible Porous-Silicon Photolithographic Process," *J. Microelectromechanical Syst.*, vol. 20, pp. 418–423, 2011.

[252] A. W. Adamson, *Physical chemistry of surfaces*. New York: John Wiley & Sons, New York, 5th ed., 1990.

[253] I. Langmuir, "The Adsorption of Gases On Plane Surfaces Of Glass, Mica And Platinum.," *J. Am. Chem. Soc.*, vol. 40, pp. 1361–1403, 1918.

[254] A. Zangwill, *Physics at Surfaces*, vol. 29. Cambridge: Cambridge University Press, 1988.

[255] S. Lowell and J. E. Shields, *Powder Surface Area and Porosity*. Dordrecht: Springer Netherlands, 1991.

[256] J. Condon, *Surface Area and Porosity Determination by Physisorption*. Amsterdam: Elsevier Science, 2006.

[257] K. S. Sing, "Assessment of Surface Area by Gas Adsorption," in *Adsorpt. by Powders Porous Solids*, pp. 237–268, Elsevier, 2nd ed., 2014.

[258] S. Brunauer, L. S. Deming, W. E. Deming, and E. Teller, "On a theory of the van der Waals adsorption of gases," *J. Am. Chem. Soc.*, vol. 62, pp. 1723–1732, 1940.

[259] F. London and M. Polanyi, "Über die atomtheoretische Deutung der Adsorptionskräfte," *Naturwissenschaften*, vol. 18, pp. 1099–1100, 1930.

[260] S. Brunauer, P. H. Emmett, and E. Teller, "Adsorption of gases in multimolecular layers," *J. Am. Chem. Soc.*, vol. 60, pp. 309–319, 1938.

[261] S. J. Gregg and K. S. W. Sing, *Adsorption, Surface Area and Porosity*. London: Academic Press, 2nd ed., 1982.

[262] L. H. Cohan, "Sorption Hysteresis and the Vapor Pressure of Concave Surfaces," *J. Am. Chem. Soc.*, vol. 60, pp. 433–435, 1938.

[263] T. D. Oulton, "The Pore Size-Surface Area Distribution of a Cracking Catalyst," *J. Phys. Colloid Chem.*, vol. 52, pp. 1296–1314, 1948.

[264] W. D. Harkins and G. Jura, "Surface of Solids. X. Extension of the Attractive Energy of a Solid into an Adjacent Liquid or Film, the Decrease of Energy with Distance, and the Thickness of Films," *J. Am. Chem. Soc.*, vol. 66, pp. 919–927, 1944.

[265] C. G. Schull, "The Determination of Pore Size Distribution from Gas Adsorption Data," *J. Am. Chem. Soc.*, vol. 70, pp. 1405–1410, 1948.

[266] E. P. Barrett, L. G. Joyner, and P. P. Halenda, "The Determination of Pore Volume and Area Distributions in Porous Substances. I. Computations from Nitrogen Isotherms," *J. Am. Chem. Soc.*, vol. 73, pp. 373–380, 1951.

[267] R. Roque-Malherbe, *Adsorption and Diffusion in Nanoporous Materials*. Boca Raton: CRC Press, 2007.

[268] C. Pierce, "Computation of Pore Sizes from Physical Adsorption Data," *J. Phys. Chem.*, vol. 57, pp. 149–152, 1953.

[269] G. Horváth and K. Kawazoe, "Method for the calculation of effective pore size distribution in molecular sieve carbon.," *J. Chem. Eng. Japan*, vol. 16, pp. 470–475, 1983.

[270] N. Seaton, J. Walton, and N. Quirke, "A new analysis method for the determination of the pore size distribution of porous carbons from nitrogen adsorption measurements," *Carbon N. Y.*, vol. 27, pp. 853–861, 1989.

[271] M. Kruk, M. Jaroniec, and A. Sayari, "Application of Large Pore MCM-41 Molecular Sieves To Improve Pore Size Analysis Using Nitrogen Adsorption Measurements," *Langmuir*, vol. 13, pp. 6267–6273, 1997.

[272] K. Morishige and N. Tateishi, "Adsorption hysteresis in ink-bottle pore," *J. Chem. Phys.*, vol. 119, pp. 2301–2306, 2003.

[273] P. I. Ravikovitch and A. V. Neimark, "Characterization of nanoporous materials from adsorption and desorption isotherms," *Colloids Surfaces A Physicochem. Eng. Asp.*, vol. 187-188, pp. 11–21, 2001.

[274] C. Lastoskie, K. E. Gubbins, and N. Quirke, "Pore size distribution analysis of microporous carbons: a density functional theory approach," *J. Phys. Chem.*, vol. 97, pp. 4786–4796, 1993.

[275] E. Runge and E. K. U. Gross, "Density-Functional Theory for Time-Dependent Systems," *Phys. Rev. Lett.*, vol. 52, pp. 997–1000, 1984.

[276] R. Car, "Unified Approach for Molecular Dynamics and Density-Functional Theory," *Phys. Rev. Lett.*, vol. 55, pp. 2471–2474, 1985.

[277] J. R. Reimers, M. J. Ford, and L. Goerigk, "Problems, successes and challenges for the application of dispersion-corrected density-functional theory combined with dispersion-based implicit solvent models to large-scale hydrophobic self-assembly and polymorphism," *Mol. Simul.*, vol. 42, pp. 494–510, 2016.

[278] M. Kruk and M. Jaroniec, "Gas Adsorption Characterization of Ordered Organic-Inorganic Nanocomposite Materials," *Chem. Mater.*, vol. 13, pp. 3169–3183, 2001.

[279] J. C. Groen, L. A. Peffer, and J. Pérez-Ramrez, "Pore size determination in modified micro- and mesoporous materials. Pitfalls and limitations in gas adsorption data analysis," *Microporous Mesoporous Mater.*, vol. 60, pp. 1–17, 2003.

[280] E. A. Ustinov, D. D. Do, and M. Jaroniec, "Equilibrium adsorption in cylindrical mesopores: a modified Broekhoff and de Boer theory versus density functional theory.," *J. Phys. Chem. B*, vol. 109, pp. 1947–1958, 2005.

[281] G. O'Halloran, *Capacitive Humidity Sensor Based on Porous Silicon.* PhD thesis, Delft University of Technology, Delft, 1999.

[282] Z. Rittersma, "Recent achievements in miniaturised humidity sensorsa review of transduction techniques," *Sensors Actuators A Phys.*, vol. 96, pp. 196–210, 2002.

[283] Z. Rittersma, *Microsensor Applications of Porous Silicon.* PhD thesis, University of Bremen, Maastricht, 1999.

[284] Z. Chen and C. Lu, "Humidity Sensors: A Review of Materials and Mechanisms," *Sens. Lett.*, vol. 3, pp. 274–295, 2005.

[285] G. Barillaro, "Porous Silicon Gas Sensing," in *Handb. Porous Silicon* (L. Canham, ed.), pp. 845–856, Zug: Springer International Publishing, 2014.

[286] J. Nie, J. Liu, N. Li, and X. Meng, "Dew point measurement using dual quartz crystal resonator sensor," *Sensors Actuators B Chem.*, vol. 246, pp. 792–799, 2017.

[287] D. Baselt, B. Fruhberger, E. Klaassen, S. Cemalovic, C. Britton, S. Patel, T. Mlsna, D. McCorkle, and B. Warmack, "Design and performance of a microcantilever-based hydrogen sensor," *Sensors Actuators B Chem.*, vol. 88, pp. 120–131, 2003.

[288] J. Stehle, O. Ambacher, A. Samarao, G. Yama, and U. Krishnamoorthy, "Study of a silicon parallel plate capacitor as a dew point sensor," in *2016 IEEE SENSORS*, pp. 1–3, 2016.

[289] J. J. Lingane, "Coulometric Analysis," *J. Am. Chem. Soc.*, vol. 67, pp. 1916–1922, 1945.

[290] B. Adhikari and S. Majumdar, "Polymers in sensor applications," *Prog. Polym. Sci.*, vol. 29, pp. 699–766, 2004.

[291] J. Miao, L. Cai, S. Zhang, J. Nah, J. Yeom, and C. Wang, "Air-Stable Humidity Sensor Using Few-Layer Black Phosphorus," *ACS Appl. Mater. Interfaces*, vol. 9, pp. 10019–10026, 2017.

[292] O. S. Wolfbeis, "Fiber-Optic Chemical Sensors and Biosensors," *Anal. Chem.*, vol. 76, pp. 3269–3284, 2004.

[293] W. Kim, A. Javey, O. Vermesh, Q. Wang, Y. Li, and H. Dai, "Hysteresis Caused by Water Molecules in Carbon Nanotube Field-Effect Transistors," *Nano Lett.*, vol. 3, pp. 193–198, 2003.

[294] B. Ding, J. Kim, Y. Miyazaki, and S. Shiratori, "Electrospun nanofibrous membranes coated quartz crystal microbalance as gas sensor for NH3 detection," *Sensors Actuators B Chem.*, vol. 101, pp. 373–380, 2004.

[295] W. Theiß, "Optical properties of porous silicon," *Surf. Sci. Rep.*, vol. 29, pp. 91–192, 1997.

[296] W. M. Haynes, ed., *Crc handbook of chemistry and physics*. CRC Press, 96th ed., 2015.

[297] G. Korotcenkov, *Handbook of Gas Sensor Materials: Properties, Advantages and Shortcomings for Applications Volume 1: Conventional Approaches*. Integrated Analytical Systems, New York: Springer New York, 2013.

[298] J. Harper and M. J. Sailor, "Detection of nitric oxide and nitrogen dioxide with photoluminescent porous silicon," *Anal. Chem.*, vol. 68, pp. 3713–3717, 1996.

[299] S. Zangooie, R. Bjorklund, and H. Arwin, "Vapor sensitivity of thin porous silicon layers," *Sensors and Actuators B-chemical*, vol. 43, pp. 168–174, 1997.

[300] J. Gao, T. Gao, and M. J. Sailor, "Porous-silicon vapor sensor based on laser interferometry," *Appl. Phys. Lett.*, vol. 77, pp. 901–903, 2000.

[301] G. Wang and H. Arwin, "Modification of vapor sensitivity in ellipsometric gas sensing by copper deposition in porous silicon," *Sensors Actuators B Chem.*, vol. 85, pp. 95–103, 2002.

[302] H. F. Arrand, T. M. Benson, A. Loni, R. Arens-Fischer, M. Kruger, M. Thonissen, H. Luth, and S. Kershaw, "Novel liquid sensor based on porous silicon optical waveguides," *Ieee Photonics Technol. Lett.*, vol. 10, pp. 1467–1469, 1998.

[303] V. Torres-Costa, "Development of interference filters based on multilayer porous silicon structures," *Mater. Sci. Eng. C*, vol. 23, pp. 1043–1046, 2003.

[304] T. Jalkanen, V. Torres-Costa, J. Salonen, M. Björkqvist, E. Makila, J. M. Martinez-Duart, and V. P. Lehto, "Optical gas sensing properties of thermally hydrocarbonized porous silicon Bragg reflectors," *Opt. Express*, vol. 17, pp. 5446–5456, 2009.

[305] S. Chan, P. M. Fauchet, Y. Li, L. J. Rothberg, and B. L. Miller, "Porous silicon microcavities for biosensing applications," *Phys. Status Solidi A-applied Res.*, vol. 182, pp. 541–546, 2000.

[306] V. Mulloni and L. Pavesi, "Porous silicon microcavities as optical chemical sensors," *Appl. Phys. Lett.*, vol. 76, pp. 2523–2525, 2000.

[307] J. Chapron, S. Alekseev, V. Lysenko, V. Zaitsev, and D. Barbier, "Analysis of interaction between chemical agents and porous Si nanostructures using optical sensing properties of infra-red Rugate filters," *Sensors Actuators B Chem.*, vol. 120, pp. 706–711, 2007.

[308] Z. Rittersma, A. Splinter, A. Bödecker, and W. Benecke, "A novel surface-micromachined capacitive porous silicon humidity sensor," *Sensors Actuators B Chem.*, vol. 68, pp. 210–217, 2000.

[309] S. J. Kim, B. H. Jeon, K. S. Choi, and N. K. Min, "Capacitive porous silicon sensors for measurement of low alcohol gas concentration at room temperature," *J. Solid State Electrochem.*, vol. 4, pp. 363–366, 2000.

[310] M. Björkqvist, J. Salonen, and E. Laine, "Humidity behavior of thermally carbonized porous silicon," *Appl. Surf. Sci.*, vol. 222, pp. 269–274, 2004.

[311] C. Betty, R. Lal, J. Yakhmi, and S. Kulshreshtha, "Time response and stability of porous silicon capacitive immunosensors," *Biosens. Bioelectron.*, vol. 22, pp. 1027–1033, 2007.

[312] L. Pancheri, C. Oton, Z. Gaburro, G. Soncini, and L. Pavesi, "Very sensitive porous silicon NO2 sensor," *Sensors Actuators B Chem.*, vol. 89, pp. 237–239, 2003.

[313] C. Baratto, E. Comini, G. Faglia, G. Sberveglieri, G. Di Francia, F. De Filippo, V. La Ferrara, L. Quercia, and L. Lancellotti, "Gas detection with a porous silicon based sensor," *Sensors Actuators B Chem.*, vol. 65, pp. 257–259, 2000.

[314] L. Boarino, C. Baratto, F. Geobaldo, G. Amato, E. Comini, A. M. Rossi, G. Faglia, G. Lerondel, and G. Sberveglieri, "NO2 monitoring

at room temperature by a porous silicon gas sensor," *Mater. Sci. Eng. B-solid State Mater. Adv. Technol.*, vol. 69, pp. 210–214, 2000.

[315] E. Massera, I. Nasti, L. Quercia, I. Rea, and G. Di Francia, "Improvement of stability and recovery time in porous-silicon-based NO2 sensor," *Sensors Actuators B Chem.*, vol. 102, pp. 195–197, 2004.

[316] G. Barillaro, A. Nannini, and F. Pieri, "APSFET: A new, porous silicon-based gas sensing device," *Sensors Actuators, B Chem.*, vol. 93, pp. 263–270, 2003.

[317] G. Barillaro, A. Nannini, F. Pieri, and L. M. Strambini, "Temperature behavior of the APSFET - A porous silicon-based FET gas sensor," *Sensors Actuators, B Chem.*, vol. 100, pp. 185–189, 2004.

[318] G. Barillaro, A. Diligenti, L. M. Strambini, E. Comini, and G. Faglia, "NO2 adsorption effects on p+ -n silicon junctions surrounded by a porous layer," *Sensors Actuators, B Chem.*, vol. 134, pp. 922–927, 2008.

[319] M. Björkqvist, J. Paski, J. Salonen, and V.-P. Lehto, "Temperature dependence of thermally-carbonized porous silicon humidity sensor," *Phys. status solidi*, vol. 202, pp. 1653–1657, 2005.

[320] J. Salonen, M. Björkqvist, and J. Paski, "Temperature-dependent electrical conductivity in thermally carbonized porous silicon," *Sensors Actuators A Phys.*, vol. 116, pp. 438–441, 2004.

[321] J. Tuura, "Temperature change in TCPSi sensors during adsorption and desorption (Unpublished work)." 2006.

Annales Universitatis Turkuensis

Turun yliopisto
University of Turku

ISBN 978-951-29-6844-2 (PRINT)
ISBN 978-951-29-6845-9 (PDF)
ISSN 0082-7002 (Print) | ISSN 2343-3175 (Online)

Painosalama Oy, Turku, Finland 2017